

Search for flavor changing neutral current interactions of the top quark in final states with a photon and additional jets in proton-proton collisions at $\sqrt{s} = 13$ TeV

A. Hayrapetyan *et al.**
(CMS Collaboration)

 (Received 11 December 2023; accepted 29 January 2024; published 5 April 2024)

A search for the production of a top quark in association with a photon and additional jets via flavor changing neutral current interactions is presented. The analysis uses proton-proton collision data recorded by the CMS detector at a center-of-mass energy of 13 TeV, corresponding to an integrated luminosity of 138 fb^{-1} . The search is performed by looking for processes where a single top quark is produced in association with a photon, or a pair of top quarks where one of the top quarks decays into a photon and an up or charm quark. Events with an electron or a muon, a photon, one or more jets, and missing transverse momentum are selected. Multivariate analysis techniques are used to discriminate signal and standard model background processes. No significant deviation is observed over the predicted background. Observed (expected) upper limits are set on the branching fractions of top quark decays: $\mathcal{B}(t \rightarrow u\gamma) < 0.95 \times 10^{-5}$ (1.20×10^{-5}) and $\mathcal{B}(t \rightarrow c\gamma) < 1.51 \times 10^{-5}$ (1.54×10^{-5}) at 95% confidence level, assuming a single nonzero coupling at a time. The obtained limit for $\mathcal{B}(t \rightarrow u\gamma)$ is similar to the current best limit, while the limit for $\mathcal{B}(t \rightarrow c\gamma)$ is significantly tighter than previous results.

DOI: [10.1103/PhysRevD.109.072004](https://doi.org/10.1103/PhysRevD.109.072004)

I. INTRODUCTION

In the standard model (SM) of particle physics, flavor changing neutral current (FCNC) interactions are not present at leading order (LO) and proceed through loop diagrams, which are strongly suppressed by the Glashow-Iliopoulos-Maiani (GIM) mechanism [1]. Because of this, the predicted branching fraction for a top quark decaying to an up or charm quark and a photon $\mathcal{B}(t \rightarrow q\gamma)$, with $q = u$ or c , is of the order of 10^{-14} [2–4]. While these branching fractions are too small to be measured by current experiments, some extensions to the SM allow for significant enhancements to them. For example, supersymmetry with R parity violation, two-Higgs doublet models, and technicolor can enhance $\mathcal{B}(t \rightarrow q\gamma)$ by many orders of magnitude compared to the SM value [5–7]. As a result, an observation of this signature would be a clear sign of physics beyond the SM.

The $tq\gamma$ FCNC interactions can be described by the effective field theory (EFT) framework in terms of dimension-six operators added to the SM Lagrangian [8]. The most general effective Lagrangian up to dimension-six operators, \mathcal{L}_{eff} , used to describe the FCNC $tq\gamma$ vertex has the following form:

$$\mathcal{L}_{\text{eff}} = e \sum_{q=u,c} \kappa_{tq\gamma} \bar{q} (\lambda_{tq\gamma}^L P_L + \lambda_{tq\gamma}^R P_R) \frac{i\sigma^{\mu\nu} q_\nu}{m_t} t A_\mu + \text{H.c.}, \quad (1)$$

where e is the electric charge of the electron, q_ν is the four-momentum of the photon, m_t is the top quark mass, $\sigma^{\mu\nu} = \frac{1}{2}[\gamma^\mu, \gamma^\nu]$, P_L and P_R are the left- and right-handed projection operators, t is the top quark field, $\lambda_{tq\gamma}^L$ and $\lambda_{tq\gamma}^R$ are the fractions of the FCNC couplings for left- and right-handed chiralities, $\bar{q} = \bar{u}$ or \bar{c} is the antiquark field, A_μ is the electromagnetic field, and H.c. refers to the Hermitian conjugate. The strengths of the FCNC couplings are denoted by $\kappa_{tq\gamma}$, which are proportional to C_{ij}/Λ^2 , where C_{ij} are the Wilson coefficients defined in Ref. [8], Λ is the energy scale of new physics, and $\kappa_{tq\gamma}$ and C_{ij} are dimensionless coefficients. In this analysis, no chirality is assumed for the FCNC interaction of $tq\gamma$, and $|\lambda_{tq\gamma}^L|^2 + |\lambda_{tq\gamma}^R|^2 = 1$. The values of $\kappa_{tq\gamma}$ vanish in the SM at tree level.

Searches for the FCNC interactions $tu\gamma$ and $tc\gamma$ have been performed by several experiments, with no evidence of signal as yet [9–14]. The latest results of a search for $tq\gamma$ FCNC couplings through single top quark production in association with a photon by the CMS experiment are $\mathcal{B}(t \rightarrow u\gamma) < 1.3 \times 10^{-4}$, and $\mathcal{B}(t \rightarrow c\gamma) < 1.7 \times 10^{-3}$ [13] at 95% confidence level (CL), based on proton-proton (pp) collisions collected at a center-of-mass energy of 8 TeV corresponding to an integrated luminosity of 19.8 fb^{-1} . The most stringent 95% CL limits to date have been obtained by

*Full author list given at the end of the article.

Published by the American Physical Society under the terms of the [Creative Commons Attribution 4.0 International license](https://creativecommons.org/licenses/by/4.0/). Further distribution of this work must maintain attribution to the author(s) and the published article's title, journal citation, and DOI. Funded by SCOAP³.

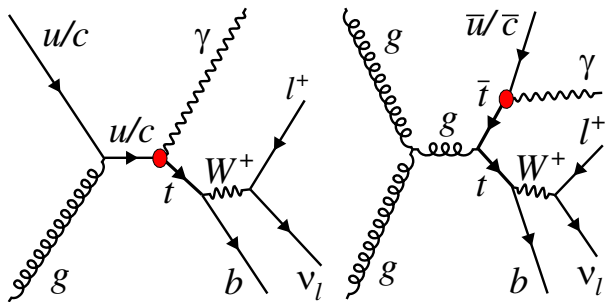


FIG. 1. LO Feynman diagrams for the production of a single top quark in association with a photon (left), and the decay of a top antiquark to a photon and a light antiquark in top quark pair production (right) via a $tq\gamma$ FCNC, where $q = u, c$. The leptonic decay of the W boson from the top quark decay is included. The charge conjugate diagrams are also included. The FCNC interaction vertex is marked as a filled red circle.

the ATLAS Collaboration at a center-of-mass energy of 13 TeV and corresponding to an integrated luminosity of 139 fb^{-1} [14]. They report 95% CL. upper limits of $\mathcal{B}(t \rightarrow u\gamma) < 0.85 \times 10^{-5}$ (1.2×10^{-5}) and $\mathcal{B}(t \rightarrow c\gamma) < 4.2 \times 10^{-5}$ (4.5×10^{-5}) for left-handed (right-handed) chiralities, respectively. This paper describes the search for $tu\gamma$ and $tc\gamma$ FCNC couplings based on the effective Lagrangian approach introduced in Eq. (1). The analysis considers both the production of a single top quark with a photon, referred to as ST, and the decay of a top quark to a photon and light-flavor quark (u or c) in top quark pair production, referred to as TT. The representative Feynman diagrams at LO for ST and TT are shown in Fig. 1.

We focus on final states where the top quark decays into a W boson and a b quark, followed by the decay of the W boson to a neutrino and an electron or muon, with electrons or muons from leptonic decays of tau leptons also being included. The data for this analysis were collected by the CMS detector between 2016–2018 in pp collisions at a center-of-mass energy of 13 TeV and correspond to an integrated luminosity of 138 fb^{-1} . Tabulated results are provided in the HEPData record for this analysis [15].

II. THE CMS DETECTOR

The central feature of the CMS apparatus is a superconducting solenoid of 6 m internal diameter, providing a magnetic field of 3.8 T. Within the solenoid volume are a silicon pixel and strip tracker, a lead tungstate crystal electromagnetic calorimeter (ECAL), and a brass and scintillator hadron calorimeter (HCAL), each composed of a barrel and two end cap sections. Forward calorimeters extend the pseudorapidity (η) coverage provided by the barrel and end cap detectors, which improves the measurement of the imbalance in transverse momentum (p_T). Muons are detected in gas-ionization chambers embedded in the steel flux-return yoke outside the solenoid. In the barrel section of the ECAL, an energy resolution of about

1% is achieved for unconverted or late-converting photons that have energies in the range of tens of GeV. The remaining barrel photons have a resolution of about 1.3% up to a pseudorapidity of $|\eta| = 1$, rising to about 2.5% at $|\eta| = 1.4$ [16]. The electron momentum is estimated by combining the energy measurement in the ECAL with the momentum measurement in the tracker. The momentum resolution for electrons with $p_T \approx 45 \text{ GeV}$ from $Z \rightarrow ee$ decays ranges from 1.6% to 5%. It is generally better in the barrel region than in the end caps, and also depends on the bremsstrahlung energy emitted by the electron as it traverses the material in front of the ECAL [17]. Muons are measured in the pseudorapidity range $|\eta| < 2.4$, with detection planes made using three technologies: drift tubes, cathode strip chambers, and resistive plate chambers. Matching muons to tracks measured in the silicon tracker results in a relative transverse momentum resolution, for muons with p_T up to 100 GeV, of 1% in the barrel and 3% in the end caps [18]. Events of interest are selected using a two-tier trigger system. The first level (L1), composed of custom hardware processors, uses information from the calorimeters and muon detectors to select events in a fixed time interval of less than $4 \mu\text{s}$ [19]. The second level, called the high-level trigger, consists of a farm of processors running a version of the full event reconstruction software optimized for fast processing, and decreases the event rate from around 100 kHz to less than 1 kHz before data storage [20]. A more detailed description of the CMS detector, together with a definition of the coordinate system used and the relevant kinematic variables, can be found in Ref. [21].

III. SIGNAL AND BACKGROUND SIMULATION

To account for the changes in conditions related to the CMS detector over the three years in which the data were taken, the data from each year are analyzed independently using the corresponding corrections and calibrations.

Signal events and background processes are simulated for each of the three data-taking years using various Monte Carlo (MC) generator packages. The signal samples corresponding to ST production associated with a photon, and $t\bar{t}$ production with an FCNC decay of one of the top quarks, are generated at LO with MadGraph 5_aMC@NLO 2.4.2 [22]. Based on the cross section calculation with the TOP++ 2.0 program [23] at next-to-next-to-LO in quantum chromodynamics (QCD) including soft-gluon resummation to next-to-next-to-leading-logarithmic order, the top quark pair production cross section is taken as 832 pb. Two signal scenarios are generated: ($\kappa_{tu\gamma} = 0.1, \kappa_{tc\gamma} = 0.0$) and ($\kappa_{tu\gamma} = 0.0, \kappa_{tc\gamma} = 0.1$), with corresponding LO ST cross sections of 0.707 and 0.100 pb, respectively, and TT cross section times FCNC branching fraction of 1.367 pb for both scenarios. The $\sigma_{\text{NLO}}/\sigma_{\text{LO}}$ K factors of 1.37 and 1.41 [24] are used to account for next-to-LO (NLO) QCD corrections for $tu\gamma$ and $tc\gamma$ couplings, respectively. Since the final state

kinematical distributions are independent of the FCNC $tq\gamma$ couplings, we only need to generate ST and TT signal samples for the two scenarios described above (and scale them as necessary).

The MadGraph 5_aMC@NLO 2.4.2 package is used to generate most of the background processes including $t\bar{t}\gamma$, $t\gamma$, Drell-Yan, $WW\gamma$, $Z\gamma + \text{jets}$, $W\gamma + \text{jets}$, and VV , where $V = W, Z$, at NLO. The single top quark production processes (t -, s -, tW -channel) and top quark pair production are generated at NLO with POWHEG 2.0 [25–27]. The simulation of signal and all background events is interfaced with PYTHIA 8.2 [28] for parton showering, fragmentation, and hadronization. The underlying event is modeled using PYTHIA 8.2 with the CUETP8M1 [29] and CP5 [30] tunes for 2016 and 2017–2018 data, respectively. The parton distribution functions (PDFs) that are used for 2016 simulation are NNPDF 3.0 [31] and for 2017/2018 simulation are NNPDF 3.1 [32].

The CMS detector response for both signal and background processes is modeled with the Geant4 program [33]. Simulated minimum-bias interactions in nearby or in the same pp bunch crossing, referred to as “pileup”, are included. Events in the simulation are reweighted to reproduce the pileup distribution observed in the data [34].

IV. EVENT RECONSTRUCTION

The particle-flow (PF) algorithm is used to reconstruct and identify the particles (photons, electrons, muons, charged and neutral hadrons) produced in the event by combining the information from various subdetectors [35]. The primary vertex (PV) is taken to be the vertex corresponding to the hardest scattering in the event, evaluated using tracking information alone, as described in Sec. 9.4.1 of Ref. [36]. In this analysis, events of interest contain one isolated charged lepton (either a muon or an electron), an isolated photon, at least one jet, and missing transverse momentum. Quality criteria are applied to improve the purity of events containing genuine leptons and photons and to help reject candidates that originate from misidentified jets or from pileup events.

Photon candidates are identified according to the presence of an energy deposit in the ECAL with no associated charged-particle tracks matched with this deposit [17]. The photon energy is obtained from the ECAL measurement. Corrections to account for the zero suppression and energy scale are applied in both simulation and data [17]. The reconstructed photons must satisfy quality criteria based on the following quantities: the relative amount of deposited energy in the ECAL and HCAL; a “shower shape” variable quantifying the lateral development of the shower [17]; separate isolation variables for charged hadrons, neutral hadrons, and photons; and a variable that quantifies whether the photon candidate is consistent with a hit in the pixel detector.

Electron reconstruction relies on a match between the clusters in the ECAL and the tracks in the tracker. The energy of an electron is estimated from the combination of electron momentum as determined by the tracker at the PV and the energy of the corresponding cluster in the ECAL including the energy sum of all the bremsstrahlung photons compatible with the electron track [17]. Electrons are required to satisfy identification criteria related to the track impact parameters with respect to the PV, the matching between the ECAL cluster and the associated track, the ratio of hadronic to electromagnetic energy deposits, and the shower shape in the ECAL. A veto on electrons originating from photon conversions is applied [17].

Muon reconstruction is based on the combination of information from the tracker and the muon system [18]. A global track fit is produced using the combined information, and the muon momentum is obtained from the track curvature. Identification criteria are based on the impact parameters with respect to the PV, the number of hits in the muon systems and the tracker, the number of matched muon detector planes, as well as the fit quality of the combined muon track.

The photon and charged lepton candidates are required to be isolated from other particles in an event. For electrons and muons (ℓ), a relative isolation variable is defined as

$$I_{\text{rel}}^{\ell} = \frac{1}{p_{\text{T}}^{\ell}} \left[\sum_{\text{charged}} p_{\text{T}} + \max \left(0, \left[\sum_{\text{neutral}} p_{\text{T}} + \sum_{\text{photons}} p_{\text{T}} \right] - p_{\text{T}}^{\text{pileup}} \right) \right], \quad (2)$$

where the sums run over the p_{T} of charged and neutral hadrons, as well as the photons, in a cone of $\Delta R < 0.3$ (0.4) centered on the electron (muon), where $\Delta R = \sqrt{(\Delta\eta)^2 + (\Delta\phi)^2}$. Here, $\Delta\eta$ is the difference in pseudorapidity, and $\Delta\phi$ is the difference in azimuthal angle between the direction of the lepton and the other particles inside the isolation cone. To reduce the pileup effects, only charged hadrons compatible with originating at the PV are taken into account. For the sums corresponding to photons and neutral hadrons, an estimate of the expected pileup contribution ($p_{\text{T}}^{\text{pileup}}$) is subtracted. For photons, three separate isolation variables, corresponding to charged hadrons, neutral hadrons, and other photons, are defined within a cone of $\Delta R < 0.3$ [17]. The effect of pileup in each variable is subtracted [37].

The muon and electron requirements, including the identification and isolations criteria mentioned above, describe the “tight” selection, and are intended to efficiently select leptons originating from the decay of gauge bosons [17,18]. A less stringent set of requirements, referred to as the “loose” selection, is also used in the analysis for the purpose of vetoing events with additional

leptons and to define a control region (CR) enriched in nongenuine leptons. The tight leptons are a subset of the loose leptons.

Jets are clustered from the PF candidates using the infrared- and collinear-safe anti- k_T algorithm [38,39] with a distance parameter of $\Delta R = 0.4$. To correct for the contributions from pileup, charged particles originating from vertices other than the PV are discarded and a correction is applied to the neutral contributions. Jet energy corrections are derived from simulation to, on average, equal the summed energy of the truth-level particles in the jet. In situ measurements of the momentum balance in dijet, γ + jet, Z + jet, and multijet events are used to account for any residual differences in the jet energy scale between data and simulation [40]. The jet energy resolution (JER) is typically 15%–20% at 30 GeV, 10% at 100 GeV, and 5% at 1 TeV [40]. Additional selection criteria are applied to each jet to remove jets potentially dominated by anomalous contributions from various subdetector components or reconstruction failures [41].

The missing transverse momentum vector (\vec{p}_T^{miss}) is computed as the negative vector p_T sum of all the PF candidates, and its magnitude is denoted as p_T^{miss} [42]. The \vec{p}_T^{miss} is modified to account for corrections to the reconstructed energy scale of jets.

V. EVENT SELECTION AND ANALYSIS STRATEGY

Events are collected with single-lepton triggers, with minimum p_T thresholds for electrons of 27 GeV in 2016 and 32 GeV in 2017 and 2018, and for muons of 24 GeV in 2016 and 27 GeV in 2017 and 2018.

Events are selected by requiring the presence of either a tight electron with $p_T > 35$ GeV and $|\eta| < 2.5$ or a tight muon with $p_T > 30$ GeV and $|\eta| < 2.4$ that matches the triggering lepton. Events with only a tight electron candidate in the ECAL barrel-end cap transition region of $1.44 < |\eta| < 1.57$ are rejected because the reconstruction of electrons in this region is suboptimal. Events are discarded if they contain an additional loose electron with $p_T > 20$ GeV, or loose muon with $p_T > 15$ GeV. Photons are required to have $p_T > 30$ GeV and $|\eta| < 1.44$, and pass the medium identification and isolation requirements [17]. Photons in the end cap region $|\eta| > 1.57$ are not considered as the signal purity is lower in this region.

For both electron and muon channels, we require $p_T^{\text{miss}} > 30$ GeV to reduce the background from events without neutrinos. In the electron channel, due to the higher probability of electrons to be misidentified as a photon, a veto on events with $81 < m_{e\gamma} < 101$ GeV is applied to suppress the contribution of $Z \rightarrow e^+e^-$ events.

Events are required to have at least one reconstructed jet with $p_T > 30$ GeV and $|\eta| < 2.7$ or $p_T > 60$ GeV and $2.7 < |\eta| < 3.0$. Higher p_T is required in the forward

region to mitigate an excess of jets caused by noise in the end cap of ECAL. The selected jets are required to be separated from the selected lepton by $\Delta R > 0.4$. The DEEPSV tagging algorithm [43] is used to identify jets originating from the hadronization of b quarks. The chosen selection requirements correspond to an efficiency of around 70% in identifying b jets and to a misidentification rate of 12% for c quark jets, and 1% for light-quark and gluon jets. The region over which the b jets can be identified increased from $|\eta| < 2.4$ in 2016 to $|\eta| < 2.5$ in 2017–2018 following an upgrade to the pixel detector [44]. The top quark is reconstructed using the lepton, the b -tagged jet, and \vec{p}_T^{miss} , where the neutrino p_T is assumed to be equal to p_T^{miss} . The longitudinal component of the neutrino momentum is obtained by constraining the invariant mass of the lepton and the neutrino to the nominal W boson mass [45], and the top quark momentum is reconstructed from the combination of the momenta of the reconstructed W boson and the b jet [46–48].

In addition to the above requirements, photons are required to be well separated from the selected lepton and jets by $\Delta R > 0.5$. This requirement helps to avoid distortion of the photon energy measurement due to the presence of close-by jets. Furthermore, it reduces the contributions of photons emitted from top quark decay products.

Two statistically independent signal regions (SRs) are defined for each lepton channel:

- (i) SR1: exactly one b -tagged jet and no additional jet ($N_j = 1$ and $N_b = 1$). This region targets the signal from FCNC ST quark production with a photon.
- (ii) SR2: at least two jets, exactly one of which is b -tagged ($N_j \geq 2$ and $N_b = 1$). This region targets TT events with the FCNC decay of one of the top quarks.

VI. BACKGROUND ESTIMATION

Several processes with identical or similar final states to the signal are sources of background for this analysis. We distinguish four different sources of background: nonprompt-photon, nonprompt-lepton, misidentified-photon, and irreducible backgrounds. Nonprompt-photon backgrounds come from events in which a jet is misidentified as a photon. This is usually the result of a high- $p_T\pi^0$ or η meson in the jet decaying to a pair of photons. Nonprompt-lepton backgrounds are from events in which the selected lepton is from the decay of a hadron. Misidentified photon backgrounds originate from events in which an electron is misidentified as a photon. Irreducible backgrounds are events in which a genuine photon and charged lepton originate from the pp collision vertex. Expected and observed event yields for all background processes are presented in Table I, where all background contributions are predicted from data except for $t\gamma$ and $VV\gamma$.

TABLE I. Estimated background yields and observed event counts for the electron and muon channels in the signal regions SR1 and SR2. The uncertainties are the statistical and systematic contributions summed in quadrature.

Process	SR1 (e channel)	SR2 (e channel)	SR1 (μ channel)	SR2 (μ channel)
$t\bar{t}\gamma$	360 ± 76	4270 ± 900	420 ± 72	5020 ± 850
$W\gamma + \text{jets}$	850 ± 130	1170 ± 210	757 ± 76	970 ± 110
$Z\gamma + \text{jets}$	366 ± 66	550 ± 150	900 ± 120	900 ± 210
$t\gamma$	288 ± 85	1030 ± 300	319 ± 93	1140 ± 340
$VV\gamma$	5 ± 3	37 ± 17	6 ± 4	38 ± 16
$\text{jet} \rightarrow \gamma$	532 ± 97	1970 ± 360	579 ± 97	2100 ± 350
$\text{jet} \rightarrow e/\mu$	650 ± 130	1100 ± 220	570 ± 110	790 ± 160
$e \rightarrow \gamma$	1050 ± 280	3090 ± 760	800 ± 210	2930 ± 730
Total	4100 ± 370	13200 ± 1300	4350 ± 320	13900 ± 1300
Data	4308	13166	4252	13530

The estimated backgrounds are described in the rest of this section.

A. Nonprompt-photon background

Nonprompt-photon events arise primarily from $W + \text{jets}$ and $t\bar{t}$ events when the jets have a high fraction of their energy deposited in the ECAL, and thus mimic prompt photons. Because the probability for jets to satisfy the photon identification criteria is not well modeled by the simulation, this source of background is estimated from data.

The SR photon requirements include selections on the charged-hadron isolation, neutral-hadron isolation, and photon isolation, as well as requirements on the shower shape and the ratio of hadronic to electromagnetic energy. These five requirements are placed at the “medium operating point” of [17] with average signal efficiency of 80%. Each of these variables also has a “loose operating point” with average signal efficiency of 90%, which is less stringent than the medium one.

We begin by using the matrix “ABCD” method, with the two axes being the charged-hadron isolation variable and the shower shape variable, which are found to be uncorrelated. The A region is the SR, containing events in which the photon candidate passes all medium selections. The B, C, and D regions are similar to the SR except for these two mentioned variables. The B and C regions contain events where either the charged-hadron isolation or the shower shape variable fails the loose selection, and the other one passes the medium selection. The D region is constructed from events that fail the loose selection of both the charged-hadron isolation and shower shape variables. An estimate of the number of nonprompt-photon events in region A (the SR) can be obtained from $N_B N_C / N_D$.

In addition to the normalization of the nonprompt-photon background in the signal region, a full set of background distributions is needed. Therefore, we also use a CR enriched in nonprompt-photons called the photonlike jet (PLJ) sample. The PLJ sample is created

by selecting events in which the photon candidate fails exactly one of the five selection criteria at the loose operating point while passing the other criteria at the medium operating point.

We then define an extrapolation factor,

$$\text{EF}(p_T) = \frac{N_{B(p_T)} N_{C(p_T)}}{N_{D(p_T)} N_{\text{PLJ}(p_T)}}, \quad (3)$$

which is calculated in p_T bins, as the fraction of nonprompt photons is known to depend on p_T . All of the events in the PLJ sample are weighted by $\text{EF}(p_T)$ to obtain the estimated distribution of nonprompt-photon events in the SR. The estimation is performed separately for each lepton channel and for each data-taking year.

The method is validated using simulation samples. In the first step, the extrapolation factors are recalculated using simulated samples. Then the contribution of the $W + \text{jets}$ sample, which is one of the main sources of nonprompt-photon background in the SR, is compared to the value estimated by the method described above for this sample. The comparison shows an agreement between 10%–15% depending on the years and lepton channels.

B. Nonprompt-lepton background

The nonprompt-lepton background contribution is estimated from data using the “tight-to-loose ratio” method [49]. A dijet CR enriched in nonprompt-lepton events is selected by requiring exactly one loose lepton, exactly one jet with $p_T > 30$ GeV and $|\eta| < 2.5$, $p_T^{\text{miss}} < 30$ GeV, $\Delta R(\ell, \text{jet}) > 0.3$, and a transverse mass of the lepton and p_T^{miss} less than 20 GeV. The last criterion is used to suppress $W + \text{jets}$ events. The p_T^{miss} requirement ensures that this CR is disjoint from the SRs. The contribution of events with prompt leptons is estimated from simulation and subtracted from the sample.

The nonprompt rate (NPR) is calculated from this sample as the fraction of events in which the selected lepton passes the tight selection. This rate is measured in bins of lepton

p_T and η and converted to a weight $w = \text{NPR}/(1 - \text{NPR})$. A second CR is defined by requiring all of the SR criteria, except that the lepton requirement is changed to select leptons that pass the loose requirement and fail the tight requirement. The contribution of events with prompt leptons is estimated from simulation and subtracted from this sample. The weight $w(p_T^\ell, \eta^\ell)$ is applied to all events in this CR to estimate the number of nonprompt-lepton events in the SR.

The method is validated in simulation using a γ + jets sample, which is the dominant source of the nonprompt-lepton background. The contribution of γ + jets events in the SR is compared to the estimate from the above method applied to the same simulated events and found to deviate by no more than 20%.

C. Misidentified-photon background

The misidentified-photon background arises from events in which an electron is misidentified as a photon. This can originate in both channels from $t\bar{t}$, diboson, and single top quark tW -channel production. In addition, $Z(\rightarrow e^+e^-)$ + jets events contribute to the electron channel.

The normalization for this background source is estimated using two CRs. The first CR has the same criteria as for the signal region, except that only the electron channel is considered and the invariant mass of the electron and photon is required to be in the range of $|m_{e\gamma} - m_Z| < 10$ GeV (the inverse of the veto used in the SR definition). The second CR also uses the SR criteria, except instead of requiring a photon and an electron, we require two electrons passing the tight selection with an invariant mass of $|m_{ee} - m_Z| < 10$ GeV. Both regions select $Z(\rightarrow e^+e^-)$ + jets events, with the second CR containing two correctly identified electrons and the first CR containing one electron misidentified as a photon. The ratio of the number of events in the first CR to the number of events in the second CR is calculated for both data and MC simulation. From these two ratios, the double ratio is calculated as

$$\text{SF}(e \rightarrow \gamma) = \frac{N_{e\gamma}(\text{data})/N_{ee}(\text{data})}{N_{e\gamma}(\text{MC})/N_{ee}(\text{MC})}, \quad (4)$$

which is applied as a scale factor to simulated background events in each SR in which the reconstructed photon is matched to a generated electron.

D. Irreducible backgrounds

Irreducible backgrounds arise from $t\bar{t}\gamma$, $W\gamma$ + jets, $Z\gamma$ + jets, $t\gamma$, and $VV\gamma$ processes. The shapes of these background sources are obtained from simulation. The normalizations for the $t\gamma$ and $VV\gamma$ processes are obtained from their respective NLO cross sections, while the normalizations for the other processes are constrained from

data using CRs. The $t\bar{t}\gamma$ CR is constructed with the same requirements as in the SRs, but with $N_j \geq 2$ and $N_b \geq 2$. A single-bin fit is made in this CR to obtain the correction factor that can be used in the SRs to correct the estimated number of $t\bar{t}\gamma$ events from MC. The $W\gamma$ + jets and $Z\gamma$ + jets CRs use the same criteria as the SRs but with $N_j \geq 1$ and $N_b = 0$ and are distinguished from each other by requiring the invariant mass of the lepton and photon to satisfy, for the electron channel, $m_{\ell\gamma} < m_Z - 10$ GeV for the $Z\gamma$ + jets CR and $m_{\ell\gamma} > m_Z + 10$ GeV for the $W\gamma$ + jets CR, and for the muon channel, $m_{\ell\gamma} < m_Z$ for the $Z\gamma$ + jets CR and $m_{\ell\gamma} > m_Z$ for the $W\gamma$ + jets CR. The reason that $Z\gamma$ + jets events are populated in the low $m_{\ell\gamma}$ region is that in many cases the selected photon is radiated off the lepton from the Z boson decay with high angular separation. The normalization of each process in the SR is corrected by scale factors obtained from a simultaneous fit of the $m_{\ell\gamma}$ distribution in the two CRs. For all three CRs, the background from other sources is estimated using the methods described above for nonprompt-photon, nonprompt-lepton, and misidentified-photon backgrounds, and from simulation for the remaining sources.

E. Summary of the backgrounds

Event yields in data and MC for all background processes are presented in Table I. The irreducible backgrounds from $t\bar{t}\gamma$, $W\gamma$ + jets, and $Z\gamma$ + jets are normalized with the control regions. The remaining irreducible backgrounds ($t\gamma$ and $VV\gamma$) are estimated from simulation. The nonprompt-photon, nonprompt-lepton, and misidentified-photon backgrounds are estimated from data.

VII. DISCRIMINATION OF SIGNAL AND BACKGROUND

To distinguish the potential FCNC signal from backgrounds, a number of discriminant variables are combined into a multivariate classification based on boosted decision trees (BDTs) [50]. Separate BDT classifiers are trained for the two signal scenarios ($tu\gamma$ and $tc\gamma$), the two SRs (SR1 and SR2), and the two channels (electron and muon), for a total of eight BDTs. The BDT input variables include photon p_T and η , lepton η , reconstructed top quark mass ($m_{\ell\nu b}$), transverse mass of the W boson defined as $m_{WT} = \sqrt{2p_T^\ell p_T^{\text{miss}}(1 - \cos \Delta\phi)}$ where $\Delta\phi$ is the difference in azimuthal angle between the lepton and \vec{p}_T^{miss} , invariant mass of the photon and non- b jet ($m_{\text{jet}+\gamma}$), p_T^{miss} , $\Delta R(\ell, \gamma)$, $\Delta R(t, \gamma)$, jet multiplicity, $\Delta R(\ell, b\text{jet})$, $\Delta R(b\text{jet}, \gamma)$. In addition, for the $tu\gamma$ signal, the lepton charge is added as an input variable, to provide sensitivity to the asymmetry between top quark and top antiquark production [51], which arises from different PDFs for the up quark and up antiquark in the colliding protons. Simulated $tu\gamma$ and $tc\gamma$ signal processes are used in conjunction with simulated

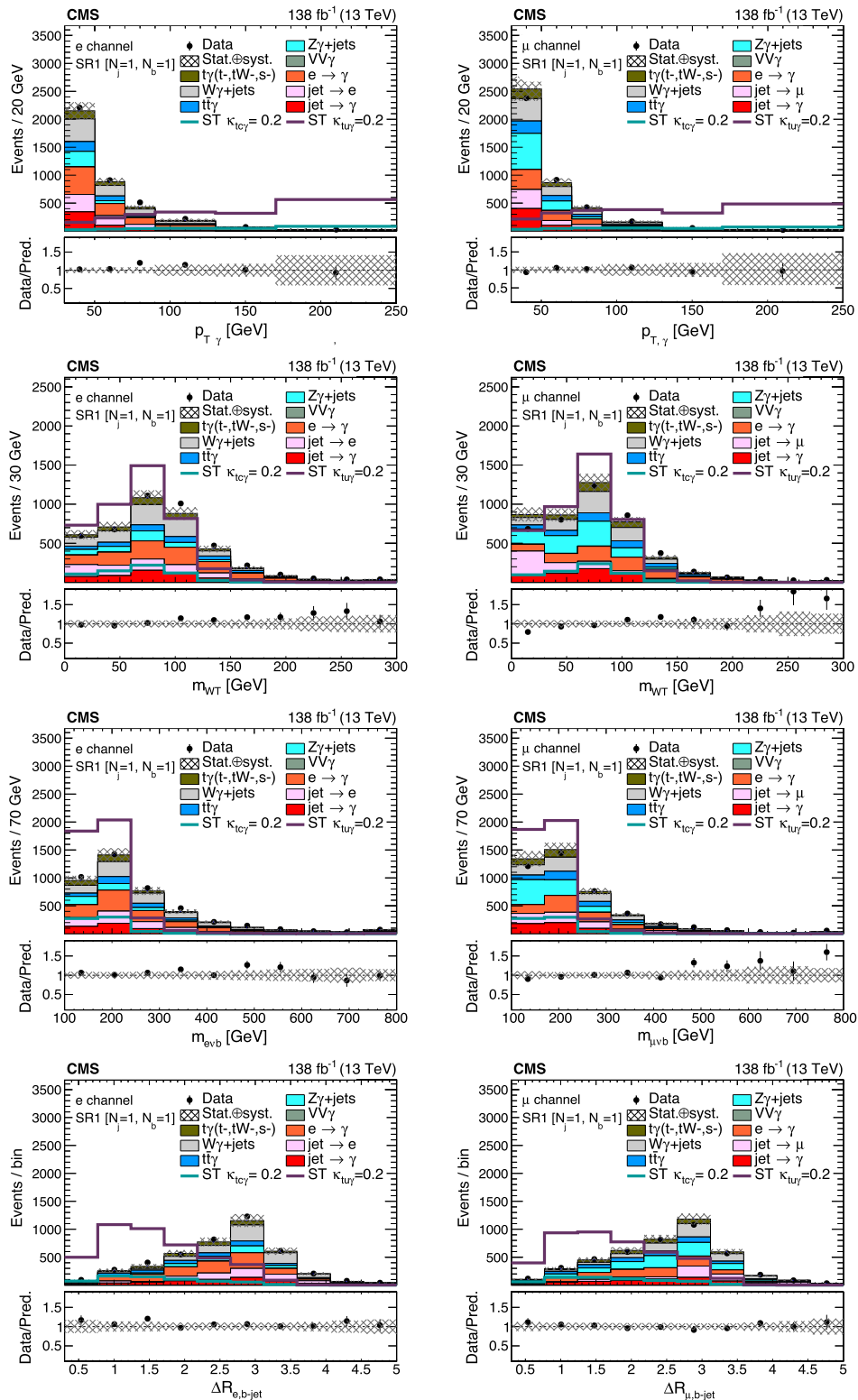


FIG. 2. From upper to lower, expected and observed distributions of photon p_T , transverse mass of W boson candidate, reconstructed top quark mass, and $\Delta R(\ell, b \text{ jet})$ for the electron (left) and muon (right) channels in SR1. For presentational purposes, the $t\bar{t}\gamma$ and $t\gamma$ signal distributions are normalized to a cross section corresponding to $\kappa_{t\mu\gamma} = \kappa_{t\gamma} = 0.2$ and are superimposed on the background expectations. The last bins include overflows. The vertical bars on the points depict the data statistical uncertainties, and the hatched bands show the combined statistical and systematic uncertainties in the estimated background processes.

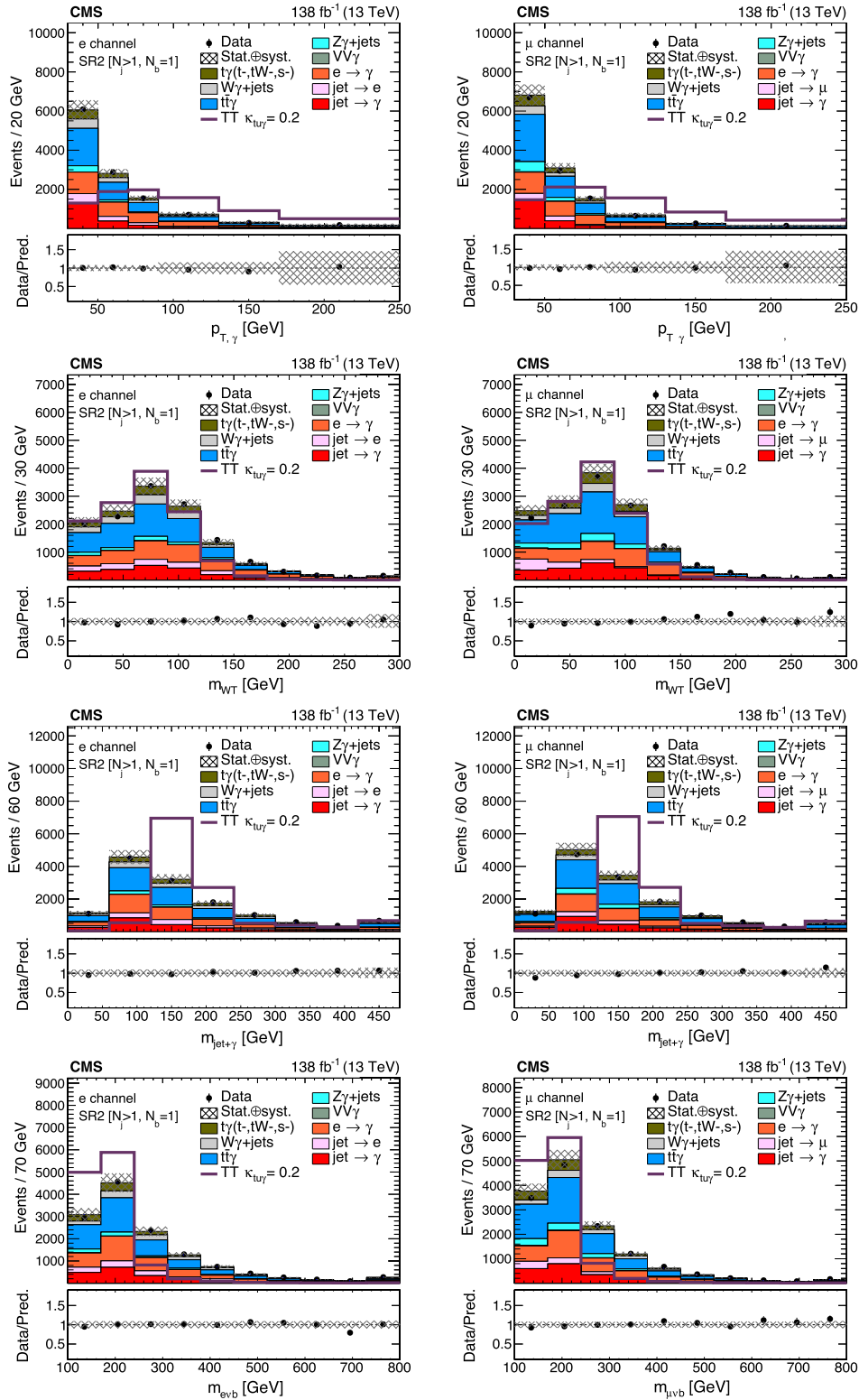


FIG. 3. From upper to lower, expected and observed distributions of photon p_T , transverse mass of W boson candidate, invariant mass of jet and photon, and reconstructed top quark mass, for the electron (left) and muon (right) channels in SR2. For presentational purposes, the $tt\gamma$ signal distributions are normalized to a cross section corresponding to $\kappa_{tt\gamma} = 0.2$ and are superimposed on the background expectations. The $tt\gamma$ distributions are not shown as they are the same as the $tt\gamma$ distributions. The last bins include overflows. The vertical bars on the points depict the data statistical uncertainties and the hatched bands show the combined statistical and systematic uncertainties in the estimated background processes.

$W\gamma$ + jets, $t\bar{t}\gamma$, $Z\gamma$ + jets, and $t\gamma$ background events to train the BDTs. The four most discriminating BDT variables for SR1 are photon p_T , $\Delta R(\ell, b \text{ jet})$, reconstructed top quark mass, and $\Delta R(t, \gamma)$, and for the SR2 they are $m_{\text{jet}+\gamma}$, photon p_T , reconstructed top quark mass, and $\Delta R(\ell, b \text{ jet})$.

The distributions for four selective discriminating BDT input variables are shown for the predicted background events and the observed data events from SR1 and SR2 in Figs. 2 and 3, respectively. The distributions from each channel are shown separately and the background events are estimated as described in Sec. VI. The figures also include the expected contribution of a $t\mu\gamma$ and $t\gamma$ signal for a coupling of $\kappa_{t\mu\gamma} = 0.2$. The output BDT distributions of the data, estimated backgrounds, and simulated signals are shown in Figs. 4 and 5 with the BDT trained to select $t\mu\gamma$ and $t\gamma$ events, respectively, for the combined 2016–2018 data-taking period. Each figure shows the distributions separated by channel and SRs. For presentational purposes,

the simulated FCNC signals are normalized to $\kappa_{t\mu\gamma} = 0.10$ and 0.01 for SR1 and SR2, respectively. A binned maximum likelihood fit is used to combine the 12 BDT output distributions from the two channels, two SRs, and three data-taking years, with systematic uncertainties incorporated as nuisance parameters for $t\mu\gamma$ and $t\gamma$ separately.

VIII. SYSTEMATIC UNCERTAINTIES

We consider an extensive list of systematic uncertainties from experimental sources, which primarily affect the background estimation, and from theoretical sources, which primarily affect the signal efficiency. The estimate of each source of uncertainty is determined by varying the relevant quantity and evaluating the effect on the yield and shape of the signal and background BDT distributions. The amount of variation is controlled by nuisance parameters in the maximum likelihood fit. We also account for

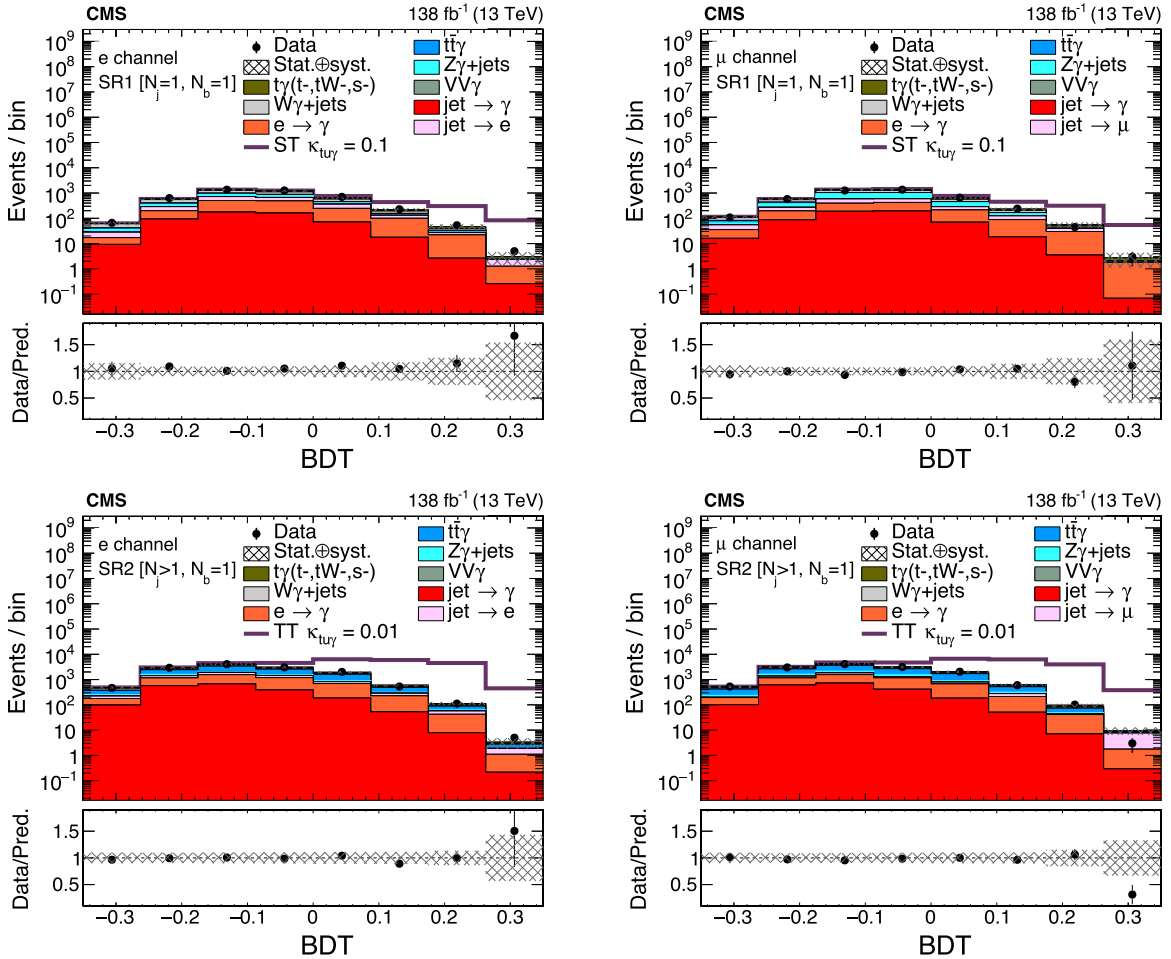


FIG. 4. The BDT output distributions for the data, the background predictions, and the expected $t\mu\gamma$ signal for electron (left) and muon (right) channels in SR1 (upper) and SR2 (lower). The signal distribution is normalized to a cross section corresponding to $\kappa_{t\mu\gamma} = 0.10$ (0.01) for ST (TT) and is stacked on the background expectations. The first bins include underflows, and the last bins include overflows. The vertical bars on the points depict the data statistical uncertainties and the hatched bands show the combined statistical and systematic uncertainties in the estimated background processes.

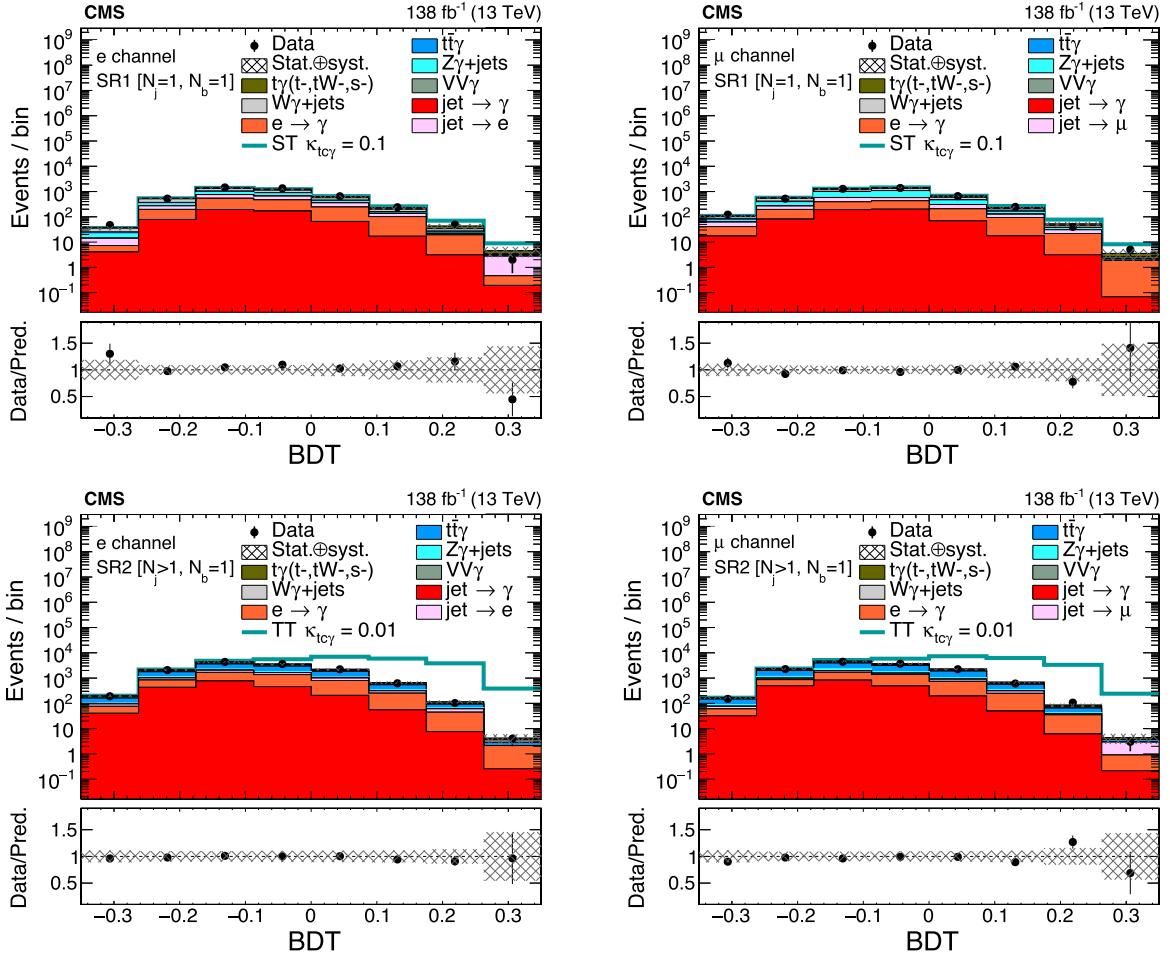


FIG. 5. The BDT output distributions for the data, the background predictions, and the expected $t\bar{c}\gamma$ signal for electron (left) and muon (right) channels in SR1 (upper) and SR2 (lower). The signal distribution is normalized to a cross section corresponding to $\kappa_{t\bar{c}\gamma} = 0.10$ (0.01) for ST (TT) and is stacked on the background expectations. The first bins include underflows, and the last bins include overflows. The vertical bars on the points depict the data statistical uncertainties and the hatched bands show the combined statistical and systematic uncertainties in the estimated background processes.

correlations among the systematic uncertainties. In particular, all uncertainties are correlated between the two SRs. Uncertainties specific to a lepton flavor are uncorrelated between the two lepton-flavor channels, while other uncertainties are correlated. The correlation between the different data-taking years is described below.

The integrated luminosity is used to normalize predictions obtained from simulation. The associated uncertainties for the data collected in 2016, 2017, and 2018 are 1.2, 2.3, and 2.5%, respectively, and are 30% correlated [52–54]. The pileup uncertainty affects the distribution of the number of pp collisions per bunch crossing. It is estimated by varying the total pp inelastic cross section by 4.6% [55] and is fully correlated for all three years.

Uncertainties in the jet energy scale are derived by recalculating the four-momentum of each jet using variations from a variety of sources, which are binned in p_T and η [40]. The variation is also propagated to \vec{p}_T^{miss} . The amount of correlation for each source is evaluated

separately across the three years. The uncertainty arising from the jet energy resolution is estimated by varying the simulated JER by its uncertainty in bins of η [40]. This variation is also propagated to \vec{p}_T^{miss} . The JER uncertainties are assumed to be uncorrelated between the three data-taking years. The uncertainty from the calibration of the photon energy scale is assessed by varying the photon energy by $\pm 0.1\%$, which is obtained from a study of $Z \rightarrow e^+e^-$ events [17].

The uncertainty associated with the data-to-simulation scale factors for the b tagging efficiency for b jets as well as the mistagging efficiencies for c jets and light-flavor and gluon jets are estimated by varying the scale factors within their uncertainties measured from a dedicated $t\bar{t}$ sample [43]. Each uncertainty is further split into correlated and uncorrelated components across the three years.

To correct the observed differences in the efficiencies between data and simulation in lepton and photon reconstruction, identification, and isolation, p_T and η

dependent scale factors with their relevant uncertainties are derived using the “tag-and-probe” method [17,18]. The impact of these sources is estimated by varying the scale factors within their uncertainties, which are propagated to the final fitting variables. The statistical component of these uncertainties is considered uncorrelated between the data-taking years while the systematic components are assumed to be fully correlated. The scale factors of leptons are derived from $Z + \text{jets}$ events but applied to the kinematic region dominated by $t\bar{t}$ events, where the lepton isolation efficiency is reduced due to a larger number of jets. Therefore, to cover the possible differences of efficiencies between these two kinematic regions, an additional uncertainty of 1% for the electron channel and 0.5% for the muon channel is applied [56].

The trigger efficiency uncertainty is assessed by varying the scale factors of each trigger within their uncertainties [17]. The resulting uncertainties are considered uncorrelated among the three years of data taking. To mitigate the gradual shift of the L1 trigger timing in the forward end cap region ($|\eta| < 2.4$) of the ECAL detector during the years 2016–2017, a correction factor is applied [19]. The correction factor and its uncertainty are used to reweight the relevant simulated events, accounting for the trigger inefficiency. The L1 inefficiency uncertainties are fully correlated between 2016 and 2017 data samples.

The uncertainty in the normalization of $WW\gamma$ is estimated from MadGraph 5_aMC@NLO to be 23%. The normalization uncertainties for the WW [57], ZZ [58], WZ [59], $t\gamma$ [60], single top quark tW -channel [61], and single top quark s -channel [62] processes are 5.8, 4.5, 40, 11, 11, and 4%, respectively, and are assigned to each background source separately. The normalization uncertainties are applied in cases where the background normalization is obtained from simulation.

The systematic uncertainty in the nonprompt-photon background estimation is calculated from three contributions. The first source is from the definition of the sideband regions in the ABCD method. To assess this uncertainty, the borders of the sideband regions are changed by 50% of their nominal values and the EFs are recalculated. The choice of 50% is made to keep the statistical uncertainty of the new sideband regions under 10%. The second source is the potential contribution of prompt-photon events in the sideband regions, which is not accounted for in the nominal method. We estimate this effect by subtracting the prompt-photon contribution using simulated events and recalculating the EFs. The third source is the EF statistical uncertainties, especially for the high- p_T photon bins. The total nonprompt-photon background uncertainty is calculated as the sum in quadrature of the three sources and the corresponding systematic uncertainty is evaluated by varying the EFs within the associated uncertainties. The uncertainty in the nonprompt-lepton background estimation is 20%, as derived from the maximum difference found

in the check of the method described in Sec. VI B. The uncertainty in the estimation of the misidentified-photon background arises from the associated scale factor uncertainties and varies within the 16%–22% range depending on the data-taking year. The background estimation uncertainties are uncorrelated between the three data-taking years.

Theoretical uncertainties arise from the choice of theoretical assumptions such as the PDFs and the renormalization and factorization scales, μ_r and μ_f , used in the cross section calculations. This affects both the calculation of the cross section and the signal efficiency. The impact of the uncertainties in the matrix elements of the generators due to μ_r and μ_f is obtained by independently varying the scales up and down by factors of 0.5 and 2. The uncertainty arising from PDFs used in the simulation is estimated by reweighting the signal events according to the NNPDF sets [63]. In addition, the uncertainty resulting from initial- and final-state radiation in the parton shower of signal events is estimated by shifting the relevant scales by a factor of 2. All of these uncertainties are correlated across the three data-taking years.

Among the systematic uncertainties, the integrated luminosity, background normalization, and nonprompt-lepton background and misidentified-photon background uncertainties affect only the rate, while the uncertainties from the remaining systematic sources affect both the shape and normalization of the BDT output distributions used in the fit.

IX. RESULTS

The data and SM prediction are in agreement within uncertainties, and no excess from FCNC contributions is observed. A modified frequentist (CL_s) criterion [64,65] in the asymptotic approximation [66] is used to compute the upper limits on the signal cross sections and branching fractions. A test statistic is defined based on the profile likelihood ratio for the compatibility of the data with background-only and signal + background hypotheses.

The limits from the combination of the electron and muon channels separately for SR1, SR2, and a combination of two SRs are presented in Table II. It summarizes the expected and observed 95% CL upper limits on the anomalous couplings $\kappa_{t\mu\gamma}$ and $\kappa_{tc\gamma}$, and the corresponding branching fractions $\mathcal{B}(t \rightarrow \mu\gamma)$ and $\mathcal{B}(t \rightarrow c\gamma)$ with NLO QCD corrections. The one and two standard deviation ($\pm 1\sigma$ and $\pm 2\sigma$) ranges of the expected limits are also presented. The largest uncertainties affecting the final likelihood fit are the statistical uncertainties from the limited number of simulated events. Among the systematic uncertainties described in Sec. VIII, the uncertainties due to the nonprompt-photon background, the normalizations of $Z\gamma + \text{jets}$ and $W\gamma + \text{jets}$, and the uncertainty arising from the misidentified-photon background have the greatest impact on the final limits. Overall, the post fit values of

TABLE II. The expected and observed 95% CL. upper limits using the CL_s criterion on the anomalous couplings $\kappa_{t\bar{u}\gamma}$, $\kappa_{t\bar{c}\gamma}$ and the corresponding branching fractions $\mathcal{B}(t \rightarrow u\gamma)$ and $\mathcal{B}(t \rightarrow c\gamma)$ from the combination of the electron and muon channels at NLO for SR1, SR2, and combined (SR1 + SR2).

		Observed limit	Expected limit	$\pm 1\sigma$ (expected limit)	$\pm 2\sigma$ (expected limit)
SR1	$\kappa_{t\bar{u}\gamma}$	12.3×10^{-3}	11.6×10^{-3}	$(9.7 - 14.4) \times 10^{-3}$	$(8.1 - 17.4) \times 10^{-3}$
	$\kappa_{t\bar{c}\gamma}$	15.3×10^{-3}	20.1×10^{-3}	$(16.9 - 24.4) \times 10^{-3}$	$(14.4 - 29.3) \times 10^{-3}$
	$\mathcal{B}(t \rightarrow u\gamma)$	3.79×10^{-5}	3.39×10^{-5}	$(2.33 - 5.16) \times 10^{-5}$	$(1.65 - 7.55) \times 10^{-5}$
	$\mathcal{B}(t \rightarrow c\gamma)$	5.85×10^{-5}	10.11×10^{-5}	$(7.13 - 14.95) \times 10^{-5}$	$(5.22 - 21.44) \times 10^{-5}$
SR2	$\kappa_{t\bar{u}\gamma}$	6.3×10^{-3}	7.5×10^{-3}	$(6.3 - 9.1) \times 10^{-3}$	$(5.5 - 11.0) \times 10^{-3}$
	$\kappa_{t\bar{c}\gamma}$	7.9×10^{-3}	8.3×10^{-3}	$(6.8 - 10.0) \times 10^{-3}$	$(6.0 - 11.8) \times 10^{-3}$
	$\mathcal{B}(t \rightarrow u\gamma)$	0.98×10^{-5}	1.41×10^{-5}	$(0.99 - 2.09) \times 10^{-5}$	$(0.75 - 3.02) \times 10^{-5}$
	$\mathcal{B}(t \rightarrow c\gamma)$	1.57×10^{-5}	1.71×10^{-5}	$(1.14 - 2.52) \times 10^{-5}$	$(0.89 - 3.51) \times 10^{-5}$
SR1 + SR2	$\kappa_{t\bar{u}\gamma}$	6.2×10^{-3}	6.9×10^{-3}	$(5.9 - 8.4) \times 10^{-3}$	$(5.1 - 10.1) \times 10^{-3}$
	$\kappa_{t\bar{c}\gamma}$	7.7×10^{-3}	7.8×10^{-3}	$(6.7 - 9.7) \times 10^{-3}$	$(5.7 - 11.5) \times 10^{-3}$
	$\mathcal{B}(t \rightarrow u\gamma)$	0.95×10^{-5}	1.20×10^{-5}	$(0.89 - 1.78) \times 10^{-5}$	$(0.64 - 2.57) \times 10^{-5}$
	$\mathcal{B}(t \rightarrow c\gamma)$	1.51×10^{-5}	1.54×10^{-5}	$(1.13 - 2.37) \times 10^{-5}$	$(0.81 - 3.32) \times 10^{-5}$

nuisance parameters deviate no more than 1 standard deviation from their initial values.

The results show significant improvements with respect to the previous CMS results at 8 TeV [13]. This is due to the addition of another signal region (SR2) as well as the electron channel, an increased signal cross section at the higher center-of-mass energy of 13 TeV, and larger integrated luminosity.

X. SUMMARY

The results of a search for flavor changing neutral current (FCNC) interactions in the top quark sector associated with the $t\bar{u}\gamma$ and $t\bar{c}\gamma$ vertices have been presented. These vertices are probed by a simultaneous evaluation of single top quark production in association with a photon and top quark pair production with one of the top quarks decaying via FCNC. The search is performed using proton-proton collisions at a center-of-mass energy of 13 TeV, corresponding to an integrated luminosity of 138 fb^{-1} , collected by the CMS detector at the LHC. The results are in agreement with the standard model prediction. Upper limits are set at 95% confidence level on the anomalous FCNC couplings of $\kappa_{t\bar{u}\gamma} < 6.2 \times 10^{-3}$ and $\kappa_{t\bar{c}\gamma} < 7.7 \times 10^{-3}$. The upper limits on the corresponding branching fractions are $\mathcal{B}(t \rightarrow u\gamma) < 0.95 \times 10^{-5}$ and $\mathcal{B}(t \rightarrow c\gamma) < 1.51 \times 10^{-5}$. The obtained limit for $\mathcal{B}(t \rightarrow u\gamma)$ is similar to the current best limit from the ATLAS experiment [14], while the limit for $\mathcal{B}(t \rightarrow c\gamma)$ is significantly tighter. The result for $\mathcal{B}(t \rightarrow c\gamma)$ benefits from the inclusion of the TT signal, which has comparable sensitivity for $\kappa_{t\bar{u}\gamma}$ and $\kappa_{t\bar{c}\gamma}$, as well as from having two independent SRs, one optimized for ST and one for TT.

ACKNOWLEDGMENTS

We congratulate our colleagues in the CERN accelerator departments for the excellent performance of the LHC and

thank the technical and administrative staffs at CERN and at other CMS institutes for their contributions to the success of the CMS effort. In addition, we gratefully acknowledge the computing centers and personnel of the Worldwide LHC Computing Grid and other centers for delivering so effectively the computing infrastructure essential to our analyses. Finally, we acknowledge the enduring support for the construction and operation of the LHC, the CMS detector, and the supporting computing infrastructure provided by the following funding agencies: SC (Armenia), BMBWF and FWF (Austria); FNRS and FWO (Belgium); CNPq, CAPES, FAPERJ, FAPERGS, and FAPESP (Brazil); MES and BNSF (Bulgaria); CERN; CAS, MoST, and NSFC (China); Minciencias (Colombia); MSES and CSF (Croatia); RIF (Cyprus); SENESCYT (Ecuador); MoER, ERC PUT and ERDF (Estonia); Academy of Finland, MEC, and HIP (Finland); CEA and CNRS/IN2P3 (France); SRNSF (Georgia); BMBF, DFG, and HGF (Germany); GSRI (Greece); NKFIH (Hungary); DAE and DST (India); Iran IPM (Iran); SFI (Ireland); INFN (Italy); MSIP and NRF (Republic of Korea); MES (Latvia); LAS (Lithuania); MOE and UM (Malaysia); BUAP, CINVESTAV, CONACYT, LNS, SEP, and UASLP-FAI (Mexico); MOS (Montenegro); MBIE (New Zealand); PAEC (Pakistan); MES and NSC (Poland); FCT (Portugal); MESTD (Serbia); MCIN/AEI and PCTI (Spain); MOSTR (Sri Lanka); Swiss Funding Agencies (Switzerland); MST (Taipei); MHESI and NSTDA (Thailand); TUBITAK and TENMAK (Turkey); NASU (Ukraine); STFC (United Kingdom); DOE and NSF (USA). Individuals have received support from the Marie-Curie program and the European Research Council and Horizon 2020 Grant, Contracts No. 675440, No. 724704, No. 752730, No. 758316, No. 765710, No. 824093, and COST Action CA16108 (European Union); the Leventis Foundation; the Alfred P. Sloan

Foundation; the Alexander von Humboldt Foundation; the Science Committee, Project No. 22r1-037 (Armenia); the Belgian Federal Science Policy Office; the Fonds pour la Formation à la Recherche dans l'Industrie et dans l'Agriculture (FRIA-Belgium); the Agentschap voor Innovatie door Wetenschap en Technologie (IWT-Belgium); the F. R. S.-FNRS and FWO (Belgium) under the “Excellence of Science—EOS”—be.h Project No. 30820817; the Beijing Municipal Science & Technology Commission, No. Z191100007219010 and Fundamental Research Funds for the Central Universities (China); the Ministry of Education, Youth and Sports (MEYS) of the Czech Republic; the Shota Rustaveli National Science Foundation, Grant FR-22-985 (Georgia); the Deutsche Forschungsgemeinschaft (DFG), under Germany’s Excellence Strategy—EXC 2121 “Quantum Universe”—390833306, and under Project No. 400140256—GRK2497; the Hellenic Foundation for Research and Innovation (HFRI), Project Number 2288 (Greece); the Hungarian Academy of Sciences, the New National Excellence Program—ÚNKP, the NKFIH Research Grants No. K 124845, No. K 124850, No. K 128713, No. K 128786, No. K 129058, No. K 131991, No. K 133046, No. K 138136, No. K 143460, No. K 143477, No. 2020-2.2.1-ED-2021-00181, and No. TKP2021-NKTA-64 (Hungary); the Council of

Science and Industrial Research, India; the Iran National Science Foundation, Iran; ICSC—National Research Center for High Performance Computing, Big Data and Quantum Computing, funded by the EU NexGeneration program (Italy); the Latvian Council of Science; the Ministry of Education and Science, Project No. 2022/WK/14, and the National Science Center, Contracts No. Opus 2021/41/B/ST2/01369 and No. 2021/43/B/ST2/01552 (Poland); the Fundação para a Ciência e a Tecnologia, Grant No. CEECIND/01334/2018 (Portugal); the National Priorities Research Program by Qatar National Research Fund; MCIN/AEI/10.13039/501100011033, ERDF “a way of making Europe”, and the Programa Estatal de Fomento de la Investigación Científica y Técnica de Excelencia María de Maeztu, Grant No. MDM-2017-0765 and Programa Severo Ochoa del Principado de Asturias (Spain); the Chulalongkorn Academic into Its 2nd Century Project Advancement Project, and the National Science, Research and Innovation Fund via the Program Management Unit for Human Resources & Institutional Development, Research and Innovation, Grant No. B37G660013 (Thailand); the Kavli Foundation; the Nvidia Corporation; the SuperMicro Corporation; the Welch Foundation, contract C-1845; and the Weston Havens Foundation (USA).

-
- [1] S. L. Glashow, J. Iliopoulos, and L. Maiani, Weak interactions with lepton-hadron symmetry, *Phys. Rev. D* **2**, 1285 (1970).
- [2] J. A. Aguilar-Saavedra, Top flavor-changing neutral interactions: Theoretical expectations and experimental detection, *Acta Phys. Pol. B* **35**, 2695 (2004), <https://www.actaphys.uj.edu.pl/R/35/11/2695/pdf>.
- [3] J. A. Aguilar-Saavedra and B. M. Nobre, Rare top decays $t \rightarrow c\gamma$, $t \rightarrow cg$, *Phys. Lett. B* **553**, 251 (2003).
- [4] F. Larios, R. Martinez, and M. A. Perez, New physics effects in the flavor-changing neutral couplings of the top quark, *Int. J. Mod. Phys. A* **21**, 3473 (2006).
- [5] G. Couture, M. Frank, and H. König, Supersymmetric QCD flavor-changing top quark decay, *Phys. Rev. D* **56**, 4213 (1997).
- [6] R. A. Diaz, R. Martinez, and J. A. Rodriguez, The rare decay $t \rightarrow c\gamma$ in the general 2HDM type III, [arXiv:hep-ph/0103307](https://arxiv.org/abs/hep-ph/0103307).
- [7] G. Lu, F. Yin, X. Wang, and L. Wan, Rare top quark decays $t \rightarrow cV$ in the top-color-assisted technicolor model, *Phys. Rev. D* **68**, 015002 (2003).
- [8] J. A. Aguilar-Saavedra, A minimal set of top anomalous couplings, *Nucl. Phys.* **B812**, 181 (2009).
- [9] F. Abe *et al.* (CDF Collaboration), Search for flavor-changing neutral current decays of the top quark in $p\bar{p}$ collisions at $\sqrt{s} = 1.8$ TeV, *Phys. Rev. Lett.* **80**, 2525 (1998).
- [10] P. Achard *et al.* (L3 Collaboration), Search for single top production at LEP, *Phys. Lett. B* **549**, 290 (2002).
- [11] F. D. Aaron *et al.* (H1 Collaboration), Search for single top quark production at HERA, *Phys. Lett. B* **678**, 450 (2009).
- [12] H. Abramowicz *et al.* (ZEUS Collaboration), Search for single-top production in ep collisions at HERA, *Phys. Lett. B* **708**, 27 (2012).
- [13] CMS Collaboration, Search for anomalous single top quark production in association with a photon in pp collisions at $\sqrt{s} = 8$ TeV, *J. High Energy Phys.* **04** (2016) 035.
- [14] ATLAS Collaboration, Search for flavour-changing neutral-current couplings between the top quark and the photon with the ATLAS detector at $\sqrt{s} = 13$ TeV, *Phys. Lett. B* **842**, 137379 (2023).
- [15] HEPData record for this analysis (2023), <http://dx.doi.org/10.17182/hepdata.129804>.
- [16] CMS Collaboration, Performance of photon reconstruction and identification with the CMS detector in proton-proton collisions at $\sqrt{s} = 8$ TeV, *J. Instrum.* **10**, P08010 (2015).
- [17] CMS Collaboration, Electron and photon reconstruction and identification with the CMS experiment at the CERN LHC, *J. Instrum.* **16**, P05014 (2021).

- [18] CMS Collaboration, Performance of the CMS muon detector and muon reconstruction with proton-proton collisions at $\sqrt{s} = 13$ TeV, *J. Instrum.* **13**, P06015 (2018).
- [19] CMS Collaboration, Performance of the CMS Level-1 trigger in proton-proton collisions at $\sqrt{s} = 13$ TeV, *J. Instrum.* **15**, P10017 (2020).
- [20] CMS Collaboration, The CMS trigger system, *J. Instrum.* **12**, P01020 (2017).
- [21] CMS Collaboration, The CMS experiment at the CERN LHC, *J. Instrum.* **3**, S08004 (2008).
- [22] J. Alwall, R. Frederix, S. Frixione, V. Hirschi, F. Maltoni, O. Mattelaer, H.-S. Shao, T. Stelzer, P. Torrielli, and M. Zaro, The automated computation of tree-level and next-to-leading order differential cross sections, and their matching to parton shower simulations, *J. High Energy Phys.* **07** (2014) 079.
- [23] M. Czakon and A. Mitov, TOP++: A program for the calculation of the top-pair cross-section at hadron colliders, *Comput. Phys. Commun.* **185**, 2930 (2014).
- [24] Y. Zhang, B. H. Li, C. S. Li, J. Gao, and H. X. Zhu, Next-to-leading order QCD predictions for $t\gamma$ associated production via model-independent flavor-changing neutral-current couplings at hadron colliders, *Phys. Rev. D* **83**, 094003 (2011).
- [25] P. Nason, A new method for combining NLO QCD with shower Monte Carlo algorithms, *J. High Energy Phys.* **11** (2004) 040.
- [26] S. Frixione, P. Nason, and C. Oleari, Matching NLO QCD computations with parton shower simulations: The POWHEG method, *J. High Energy Phys.* **11** (2007) 070.
- [27] S. Alioli, P. Nason, C. Oleari, and E. Re, A general framework for implementing NLO calculations in shower Monte Carlo programs: The POWHEG BOX, *J. High Energy Phys.* **06** (2010) 043.
- [28] T. Sjöstrand, S. Ask, J. R. Christiansen, R. Corke, N. Desai, P. Ilten, S. Mrenna, S. Prestel, C. O. Rasmussen, and P. Z. Skands, An introduction to PYTHIA 8.2, *Comput. Phys. Commun.* **191**, 159 (2015).
- [29] CMS Collaboration, Event generator tunes obtained from underlying event and multiparton scattering measurements, *Eur. Phys. J. C* **76**, 155 (2016).
- [30] CMS Collaboration, Extraction and validation of a new set of CMS PYTHIA 8 tunes from underlying-event measurements, *Eur. Phys. J. C* **80**, 4 (2020).
- [31] R. D. Ball, V. Bertone, S. Carrazza, C. S. Deans, L. Del Debbio, S. Forte, A. Guffanti, N. P. Hartland, J. I. Latorre, J. Rojo, and M. Ubiali (NNPDF Collaboration), Parton distributions for the LHC run II, *J. High Energy Phys.* **04** (2015) 040.
- [32] R. D. Ball, V. Bertone, S. Carrazza, L. Del Debbio, S. Forte, P. Groth-Merrild, A. Guffanti, N. P. Hartland, Z. Kassabov, J. I. Latorre, E. R. Nocera, J. Rojo, L. Rottoli, E. Slade, and M. Ubiali (NNPDF Collaboration), Parton distributions from high-precision collider data, *Eur. Phys. J. C* **77**, 663 (2017).
- [33] S. Agostinelli *et al.* (GEANT4 Collaboration), Geant4—a simulation toolkit, *Nucl. Instrum. Methods Phys. Res., Sect. A* **506**, 250 (2003).
- [34] CMS Collaboration, Measurement of the inelastic proton-proton cross section at $\sqrt{s} = 13$ TeV, *J. High Energy Phys.* **07** (2018) 161.
- [35] CMS Collaboration, Particle-flow reconstruction and global event description with the CMS detector, *J. Instrum.* **12**, P10003 (2017).
- [36] CMS Collaboration, Technical proposal for the phase-II upgrade of the compact muon solenoid, CMS Technical Proposal, Reports No. CERN-LHCC-2015-010, No. CMS-TDR-15-02, 2015.
- [37] CMS Collaboration, Performance of electron reconstruction and selection with the CMS detector in proton-proton collisions at $\sqrt{s} = 8$ TeV, *J. Instrum.* **10**, P06005 (2015).
- [38] M. Cacciari, G. P. Salam, and G. Soyez, The anti- k_T jet clustering algorithm, *J. High Energy Phys.* **04** (2008) 063.
- [39] M. Cacciari, G. P. Salam, and G. Soyez, FastJet user manual, *Eur. Phys. J. C* **72**, 1896 (2012).
- [40] CMS Collaboration, Jet energy scale and resolution in the CMS experiment in pp collisions at 8 TeV, *J. Instrum.* **12**, P02014 (2017).
- [41] CMS Collaboration, Jet algorithms performance in 13 TeV data, CMS Physics Analysis Summary, Report No. CMS-PAS-JME-16-003, 2017, <https://cds.cern.ch/record/2256875>.
- [42] CMS Collaboration, Performance of missing transverse momentum reconstruction in proton-proton collisions at $\sqrt{s} = 13$ TeV using the CMS detector, *J. Instrum.* **14**, P07004 (2019).
- [43] CMS Collaboration, Identification of heavy-flavour jets with the CMS detector in pp collisions at 13 TeV, *J. Instrum.* **13**, P05011 (2018).
- [44] B. Vormwald on behalf of the CMS Collaboration, The CMS Phase-I pixel detector—experience and lessons learned from two years of operation, *J. Instrum.* **14**, C07008 (2019).
- [45] R. L. Workman *et al.* (Particle Data Group), Review of particle physics, *Prog. Theor. Exp. Phys.* **2022**, 083C01 (2022).
- [46] V. M. Abazov *et al.* (D0 Collaboration), Observation of single top-quark production, *Phys. Rev. Lett.* **103**, 092001 (2009).
- [47] T. Aaltonen *et al.* (CDF Collaboration), Observation of electroweak single top-quark production, *Phys. Rev. Lett.* **103**, 092002 (2009).
- [48] CMS Collaboration, Measurement of the t -channel single top quark production cross section in pp collisions at $\sqrt{s} = 7$ TeV, *Phys. Rev. Lett.* **107**, 091802 (2011).
- [49] CMS Collaboration, Search for new physics with same-sign isolated dilepton events with jets and missing transverse energy at the LHC, *J. High Energy Phys.* **06** (2011) 077.
- [50] A. Hoecker, P. Speckmayer, J. Stelzer, J. Therhaag, E. von Toerne, and H. Voss, TMVA: Toolkit for multivariate data analysis, *Proc. Sci.*, ACAT (2007) 040 [arXiv:physics/0703039].
- [51] S. Khatibi and M. Mohammadi Najafabadi, Probing the anomalous FCNC interactions in top-higgs boson final state and the charge ratio approach, *Phys. Rev. D* **89**, 054011 (2014).
- [52] CMS Collaboration, Precision luminosity measurement in proton-proton collisions at $\sqrt{s} = 13$ TeV in 2015 and 2016 at CMS, *Eur. Phys. J. C* **81**, 800 (2021).
- [53] CMS Collaboration, CMS luminosity measurement for the 2017 data-taking period at $\sqrt{s} = 13$ TeV, CMS Physics

- Analysis Summary, Report No. CMS-PAS-LUM-17-004, 2018, <https://cds.cern.ch/record/2621960>.
- [54] CMS Collaboration, CMS luminosity measurement for the 2018 data-taking period at $\sqrt{s} = 13$ TeV, CMS Physics Analysis Summary, Report No. CMS-PAS-LUM-18-002, 2019, <https://cds.cern.ch/record/2676164>.
- [55] CMS Collaboration, Pileup mitigation at CMS in 13 TeV data, *J. Instrum.* **15**, P09018 (2020).
- [56] CMS Collaboration, Measurement of the Higgs boson production rate in association with top quarks in final states with electrons, muons, and hadronically decaying tau leptons at $\sqrt{s} = 13$ TeV, *Eur. Phys. J. C* **81**, 378 (2021).
- [57] CMS Collaboration, W^+W^- boson pair production in proton-proton collisions at $\sqrt{s} = 13$ TeV, *Phys. Rev. D* **102**, 092001 (2020).
- [58] CMS Collaboration, Measurements of $pp \rightarrow ZZ$ production cross sections and constraints on anomalous triple gauge couplings at $\sqrt{s} = 13$ TeV, *Eur. Phys. J. C* **81**, 200 (2021).
- [59] CMS Collaboration, Measurements of production cross sections of WZ and same-sign WW boson pairs in association with two jets in proton-proton collisions at $\sqrt{s} = 13$ TeV, *Phys. Lett. B* **809**, 135710 (2020).
- [60] ATLAS Collaboration, Observation of single-top-quark production in association with a photon using the ATLAS detector, *Phys. Rev. Lett.* **131**, 181901 (2023).
- [61] CMS Collaboration, Measurement of the production cross section for single top quarks in association with W bosons in proton-proton collisions at $\sqrt{s} = 13$ TeV, *J. High Energy Phys.* **10** (2018) 117.
- [62] N. Kidonakis, Theoretical results for electroweak-boson and single-top production, *Proc. Sci. DIS2015* (2015) 170.
- [63] J. Butterworth *et al.*, PDF4LHC recommendations for LHC Run II, *J. Phys. G* **43**, 023001 (2016).
- [64] A. L. Read, Presentation of search results: The CL_s technique, *J. Phys. G* **28**, 2693 (2002).
- [65] T. Junk, Confidence level computation for combining searches with small statistics, *Nucl. Instrum. Methods Phys. Res., Sect. A* **434**, 435 (1999).
- [66] G. Cowan, K. Cranmer, E. Gross, and O. Vitells, Asymptotic formulae for likelihood-based tests of new physics, *Eur. Phys. J. C* **71**, 1554 (2011); **73**, 2501(E) (2013).

A. Hayrapetyan,¹ A. Tumasyan,^{1,b} W. Adam,² J. W. Andrejkovic,² T. Bergauer,² S. Chatterjee,² K. Damanakis,² M. Dragicvic,² A. Escalante Del Valle,² P. S. Hussain,² M. Jeitler,^{2,c} N. Krammer,² D. Liko,² I. Mikulec,² J. Schieck,^{2,c} R. Schöfbeck,² D. Schwarz,² M. Sonawane,² S. Templ,² W. Waltenberger,² C.-E. Wulz,^{2,c} M. R. Darwish,^{3,d} T. Janssen,³ P. Van Mechelen,³ E. S. Bols,⁴ J. D'Hondt,⁴ S. Dansana,⁴ A. De Moor,⁴ M. Delcourt,⁴ H. El Faham,⁴ S. Lowette,⁴ I. Makarenko,⁴ D. Müller,⁴ A. R. Sahasransu,⁴ S. Tavernier,⁴ M. Tytgat,^{4,e} S. Van Putte,⁴ D. Vannerom,⁴ B. Clerbaux,⁵ G. De Lentdecker,⁵ L. Favart,⁵ D. Hohov,⁵ J. Jaramillo,⁵ A. Khalilzadeh,⁵ K. Lee,⁵ M. Mahdavihorrani,⁵ A. Malara,⁵ S. Paredes,⁵ L. Pétré,⁵ N. Postiau,⁵ L. Thomas,⁵ M. Vanden Bemden,⁵ C. Vander Velde,⁵ P. Vanlaer,⁵ M. De Coen,⁶ D. Dobur,⁶ Y. Hong,⁶ J. Knolle,⁶ L. Lambrecht,⁶ G. Mestdach,⁶ C. Rendón,⁶ A. Samalan,⁶ K. Skovpen,⁶ N. Van Den Bossche,⁶ L. Wezenbeek,⁶ A. Benecke,⁷ G. Bruno,⁷ C. Caputo,⁷ C. Delaere,⁷ I. S. Donertas,⁷ A. Giammanco,⁷ K. Jaffel,⁷ Sa. Jain,⁷ V. Lemaître,⁷ J. Lidrych,⁷ P. Mastrapasqua,⁷ K. Mondal,⁷ T. T. Tran,⁷ S. Wertz,⁷ G. A. Alves,⁸ E. Coelho,⁸ C. Hensel,⁸ T. Menezes De Oliveira,⁸ A. Moraes,⁸ P. Rebello Teles,⁸ M. Soeiro,⁸ W. L. Aldá Júnior,⁹ M. Alves Gallo Pereira,⁹ M. Barroso Ferreira Filho,⁹ H. Brandao Malbouisson,⁹ W. Carvalho,⁹ J. Chinellato,^{9,f} E. M. Da Costa,⁹ G. G. Da Silveira,^{9,g} D. De Jesus Damiao,⁹ S. Fonseca De Souza,⁹ J. Martins,^{9,h} C. Mora Herrera,⁹ K. Mota Amarilo,⁹ L. Mundim,⁹ H. Nogima,⁹ A. Santoro,⁹ A. Sznajder,⁹ M. Thiel,⁹ A. Vilela Pereira,⁹ C. A. Bernardes,^{10,g} L. Calligaris,¹⁰ T. R. Fernandez Perez Tomei,¹⁰ E. M. Gregores,¹⁰ P. G. Mercadante,¹⁰ S. F. Novaes,¹⁰ B. Orzari,¹⁰ Sandra S. Padula,¹⁰ A. Aleksandrov,¹¹ G. Antchev,¹¹ R. Hadjiiska,¹¹ P. Iaydjiev,¹¹ M. Misheva,¹¹ M. Shopova,¹¹ G. Sultanov,¹¹ A. Dimitrov,¹² L. Litov,¹² B. Pavlov,¹² P. Petkov,¹² A. Petrov,¹² E. Shumka,¹² S. Keshri,¹³ S. Thakur,¹³ T. Cheng,¹⁴ Q. Guo,¹⁴ T. Javaid,¹⁴ M. Mittal,¹⁴ L. Yuan,¹⁴ G. Bauer,^{15,i,j} Z. Hu,¹⁵ J. Liu,¹⁵ K. Yi,^{15,i,k} G. M. Chen,^{16,l} H. S. Chen,^{16,l} M. Chen,^{16,l} F. Iemmi,¹⁶ C. H. Jiang,¹⁶ A. Kapoor,^{16,m} H. Liao,¹⁶ Z.-A. Liu,^{16,n} F. Monti,¹⁶ M. A. Shahzad,^{16,l} R. Sharma,^{16,o} J. N. Song,^{16,n} J. Tao,¹⁶ C. Wang,^{16,l} J. Wang,¹⁶ Z. Wang,^{16,l} H. Zhang,¹⁶ A. Agapitos,¹⁷ Y. Ban,¹⁷ A. Levin,¹⁷ C. Li,¹⁷ Q. Li,¹⁷ Y. Mao,¹⁷ S. J. Qian,¹⁷ X. Sun,¹⁷ D. Wang,¹⁷ H. Yang,¹⁷ L. Zhang,¹⁷ C. Zhou,¹⁷ Z. You,¹⁸ N. Lu,¹⁹ X. Gao,^{20,p} D. Leggat,²⁰ H. Okawa,²⁰ Y. Zhang,²⁰ Z. Lin,²¹ C. Lu,²¹ M. Xiao,²¹ C. Avila,²² D. A. Barbosa Trujillo,²² A. Cabrera,²² C. Florez,²² J. Fraga,²² J. A. Reyes Vega,²² J. Mejia Guisao,²³ F. Ramirez,²³ M. Rodriguez,²³ J. D. Ruiz Alvarez,²³ D. Giljanovic,²⁴ N. Godinovic,²⁴ D. Lelas,²⁴ A. Sculac,²⁴ M. Kovac,²⁵ T. Sculac,²⁵ P. Bargassa,²⁶ V. Brigljevic,²⁶ B. K. Chitroda,²⁶ D. Ferencek,²⁶ S. Mishra,²⁶ A. Starodumov,^{26,q} T. Susa,²⁶ A. Attikis,²⁷ K. Christoforou,²⁷ S. Konstantinou,²⁷ J. Mousa,²⁷ C. Nicolaou,²⁷

F. Ptochos²⁷, P. A. Razis²⁷, H. Rykaczewski²⁷, H. Saka²⁷, A. Stepennov²⁷, M. Finger²⁸, M. Finger Jr.²⁸,
A. Kveton²⁸, E. Ayala²⁹, E. Carrera Jarrin³⁰, A. A. Abdelalim^{31,r,s}, E. Salama^{31,t,u}, M. Abdullah Al-Mashad³²,
M. A. Mahmoud³², R. K. Dewanjee^{33,v}, K. Ehataht³³, M. Kadastik³³, T. Lange³³, S. Nandan³³, C. Nielsen³³,
J. Pata³³, M. Raidal³³, L. Tani³³, C. Veelken³³, H. Kirschenmann³⁴, K. Osterberg³⁴, M. Voutilainen³⁴,
S. Bharthuar³⁵, E. Brücken³⁵, F. Garcia³⁵, J. Havukainen³⁵, K. T. S. Kallonen³⁵, R. Kinnunen³⁵, T. Lampén³⁵,
K. Lassila-Perini³⁵, S. Lehti³⁵, T. Lindén³⁵, M. Lotti³⁵, L. Martikainen³⁵, M. Myllymäki³⁵, M. m. Rantanen³⁵,
H. Siikonen³⁵, E. Tuominen³⁵, J. Tuominiemi³⁵, P. Luukka³⁶, H. Petrow³⁶, T. Tuuva^{36,a}, M. Besancon³⁷,
F. Couderc³⁷, M. Dejardin³⁷, D. Denegri³⁷, J. L. Faure³⁷, F. Ferri³⁷, S. Ganjour³⁷, P. Gras³⁷,
G. Hamel de Monchenault³⁷, V. Lohezic³⁷, J. Malcles³⁷, J. Rander³⁷, A. Rosowsky³⁷, M. Ö. Sahin³⁷,
A. Savoy-Navarro^{37,w}, P. Simkina³⁷, M. Titov³⁷, M. Tornago³⁷, C. Baldenegro Barrera³⁸, F. Beaudette³⁸,
A. Buchot Perraguin³⁸, P. Busson³⁸, A. Cappati³⁸, C. Charlot³⁸, F. Damas³⁸, O. Davignon³⁸, A. De Wit³⁸,
G. Falmagne³⁸, B. A. Fontana Santos Alves³⁸, S. Ghosh³⁸, A. Gilbert³⁸, R. Granier de Cassagnac³⁸, A. Hakimi³⁸,
B. Harikrishnan³⁸, L. Kalipoliti³⁸, G. Liu³⁸, J. Motta³⁸, M. Nguyen³⁸, C. Ochando³⁸, L. Portales³⁸,
R. Salerno³⁸, U. Sarkar³⁸, J. B. Sauvan³⁸, Y. Sirois³⁸, A. Tarabini³⁸, E. Vernazza³⁸, A. Zabi³⁸, A. Zghiche³⁸,
J.-L. Agram^{39,x}, J. Andrea³⁹, D. Apparú³⁹, D. Bloch³⁹, J.-M. Brom³⁹, E. C. Chabert³⁹, C. Collard³⁹, S. Falke³⁹,
U. Goerlach³⁹, C. Grimault³⁹, R. Haerberle³⁹, A.-C. Le Bihan³⁹, G. Saha³⁹, M. A. Sessini³⁹, P. Van Hove³⁹,
S. Beauceron⁴⁰, B. Blancon⁴⁰, G. Boudoul⁴⁰, N. Chanon⁴⁰, J. Choi⁴⁰, D. Contardo⁴⁰, P. Depasse⁴⁰,
C. Dozen^{40,y}, H. El Mamouni⁴⁰, J. Fay⁴⁰, S. Gascon⁴⁰, M. Gouzevitch⁴⁰, C. Greenberg⁴⁰, G. Grenier⁴⁰, B. Ille⁴⁰,
I. B. Laktineh⁴⁰, M. Lethuillier⁴⁰, L. Mirabito⁴⁰, S. Perries⁴⁰, A. Purohit⁴⁰, M. Vander Donckt⁴⁰, P. Verdier⁴⁰,
J. Xiao⁴⁰, D. Chokheli⁴¹, I. Lomidze⁴¹, Z. Tsamalaidze^{41,q}, V. Botta⁴², L. Feld⁴², K. Klein⁴², M. Lipinski⁴²,
D. Meuser⁴², A. Pauls⁴², N. Röwert⁴², M. Teroerde⁴², S. Diekmann⁴³, A. Dodonova⁴³, N. Eich⁴³, D. Eliseev⁴³,
F. Engelke⁴³, M. Erdmann⁴³, P. Fackeldey⁴³, B. Fischer⁴³, T. Hebbeker⁴³, K. Hoepfner⁴³, F. Ivone⁴³,
A. Jung⁴³, M. y. Lee⁴³, L. Mastrolorenzo⁴³, M. Merschmeyer⁴³, A. Meyer⁴³, S. Mukherjee⁴³, D. Noll⁴³,
A. Novak⁴³, F. Nowotny⁴³, A. Pozdnyakov⁴³, Y. Rath⁴³, W. Redjeb⁴³, F. Rehm⁴³, H. Reithler⁴³, V. Sarkisovi⁴³,
A. Schmidt⁴³, A. Sharma⁴³, J. L. Spah⁴³, A. Stein⁴³, F. Torres Da Silva De Araujo^{43,z}, L. Vigilante⁴³,
S. Wiedenbeck⁴³, S. Zaleski⁴³, C. Dziwok⁴⁴, G. Flügge⁴⁴, W. Haj Ahmad^{44,aa}, T. Kress⁴⁴, A. Nowack⁴⁴,
O. Pooth⁴⁴, A. Stahl⁴⁴, T. Ziemons⁴⁴, A. Zotz⁴⁴, H. Aarup Petersen⁴⁵, M. Aldaya Martin⁴⁵, J. Alimena⁴⁵,
S. Amoroso⁴⁵, Y. An⁴⁵, S. Baxter⁴⁵, M. Bayatmakou⁴⁵, H. Becerril Gonzalez⁴⁵, O. Behnke⁴⁵, A. Belvedere⁴⁵,
S. Bhattacharya⁴⁵, F. Blekman^{45,bb}, K. Borrás^{45,cc}, D. Brunner⁴⁵, A. Campbell⁴⁵, A. Cardini⁴⁵, C. Cheng⁴⁵,
F. Colombina⁴⁵, S. Consuegra Rodríguez⁴⁵, G. Correia Silva⁴⁵, M. De Silva⁴⁵, G. Eckerlin⁴⁵, D. Eckstein⁴⁵,
L. I. Estevez Banos⁴⁵, O. Filatov⁴⁵, E. Gallo^{45,bb}, A. Geiser⁴⁵, A. Giraldi⁴⁵, G. Greau⁴⁵, V. Guglielmi⁴⁵,
M. Guthoff⁴⁵, A. Hinzmann⁴⁵, A. Jafari^{45,dd}, L. Jeppe⁴⁵, N. Z. Jomhari⁴⁵, B. Kaech⁴⁵, M. Kasemann⁴⁵,
H. Kaveh⁴⁵, C. Kleinwort⁴⁵, R. Kogler⁴⁵, M. Komm⁴⁵, D. Krücker⁴⁵, W. Lange⁴⁵, D. Leyva Pernia⁴⁵,
K. Lipka^{45,ee}, W. Lohmann^{45,ff}, R. Mankel⁴⁵, I.-A. Melzer-Pellmann⁴⁵, M. Mendizabal Morentin⁴⁵, J. Metwally⁴⁵,
A. B. Meyer⁴⁵, G. Milella⁴⁵, A. Mussgiller⁴⁵, L. P. NAIR⁴⁵, A. Nürnberg⁴⁵, Y. Otari⁴⁵, J. Park⁴⁵,
D. Pérez Adán⁴⁵, E. Ranken⁴⁵, A. Raspereza⁴⁵, B. Ribeiro Lopes⁴⁵, J. Rübenach⁴⁵, A. Saggio⁴⁵, M. Scham^{45,gg},
S. Schnake^{45,cc}, P. Schütze⁴⁵, C. Schwanenberger^{45,bb}, D. Selivanova⁴⁵, M. Shchedrolosiev⁴⁵,
R. E. Sosa Ricardo⁴⁵, D. Stafford⁴⁵, F. Vazzoler⁴⁵, A. Ventura Barroso⁴⁵, R. Walsh⁴⁵, Q. Wang⁴⁵, Y. Wen⁴⁵,
K. Wichmann⁴⁵, L. Wiens^{45,cc}, C. Wissing⁴⁵, Y. Yang⁴⁵, A. Zimmermann Castro Santos⁴⁵, A. Albrecht⁴⁶,
S. Albrecht⁴⁶, M. Antonello⁴⁶, S. Bein⁴⁶, L. Benato⁴⁶, M. Bonanomi⁴⁶, P. Connor⁴⁶, M. Eich⁴⁶, K. El Morabit⁴⁶,
Y. Fischer⁴⁶, A. Fröhlich⁴⁶, C. Garbers⁴⁶, E. Garutti⁴⁶, A. Grohsjean⁴⁶, M. Hajheidari⁴⁶, J. Haller⁴⁶,
H. R. Jabusch⁴⁶, G. Kasieczka⁴⁶, P. Keicher⁴⁶, R. Klanner⁴⁶, W. Korcari⁴⁶, T. Kramer⁴⁶, V. Kutzner⁴⁶, F. Labe⁴⁶,
J. Lange⁴⁶, A. Lobanov⁴⁶, C. Matthies⁴⁶, A. Mehta⁴⁶, L. Moureaux⁴⁶, M. Mrowietz⁴⁶, A. Nigamova⁴⁶,
Y. Nissan⁴⁶, A. Paasch⁴⁶, K. J. Pena Rodriguez⁴⁶, T. Quadfasel⁴⁶, B. Raciti⁴⁶, M. Rieger⁴⁶, D. Savoio⁴⁶,
J. Schindler⁴⁶, P. Schleper⁴⁶, M. Schröder⁴⁶, J. Schwandt⁴⁶, M. Sommerhalder⁴⁶, H. Stadié⁴⁶, G. Steinbrück⁴⁶,
A. Tews⁴⁶, M. Wolf⁴⁶, S. Brommer⁴⁷, M. Burkart⁴⁷, E. Butz⁴⁷, T. Chwalek⁴⁷, A. Dierlamm⁴⁷, A. Droll⁴⁷,
N. Faltermann⁴⁷, M. Giffels⁴⁷, A. Gottmann⁴⁷, F. Hartmann^{47,hh}, R. Hofsaess⁴⁷, M. Horzela⁴⁷, U. Husemann⁴⁷,
J. Kieseler⁴⁷, M. Klute⁴⁷, R. Koppenhöfer⁴⁷, J. M. Lawhorn⁴⁷, M. Link⁴⁷, A. Lintuluoto⁴⁷, S. Maier⁴⁷,
S. Mitra⁴⁷, M. Mormile⁴⁷, Th. Müller⁴⁷, M. Neukum⁴⁷, M. Oh⁴⁷, M. Presilla⁴⁷, G. Quast⁴⁷, K. Rabbertz⁴⁷

B. Regnery⁴⁷, N. Shadskiy⁴⁷, I. Shvetsov⁴⁷, H. J. Simonis⁴⁷, N. Trevisani⁴⁷, R. Ulrich⁴⁷, J. van der Linden⁴⁷, R. F. Von Cube⁴⁷, M. Wassmer⁴⁷, S. Wieland⁴⁷, F. Wittig⁴⁷, R. Wolf⁴⁷, S. Wunsch⁴⁷, X. Zuo⁴⁷, G. Anagnostou⁴⁸, P. Assiouras⁴⁸, G. Daskalakis⁴⁸, A. Kyriakis⁴⁸, A. Papadopoulos⁴⁸, A. Stakia⁴⁸, P. Kontaxakis⁴⁹, G. Melachroinos⁴⁹, A. Panagiotou⁴⁹, I. Papavergou⁴⁹, I. Paraskevas⁴⁹, N. Saoulidou⁴⁹, K. Theofilatos⁴⁹, E. Tziaferi⁴⁹, K. Vellidis⁴⁹, I. Zisopoulos⁴⁹, G. Bakas⁵⁰, T. Chatzistavrou⁵⁰, G. Karapostoli⁵⁰, K. Kousouris⁵⁰, I. Papakrivopoulos⁵⁰, E. Siamarkou⁵⁰, G. Tsiopolitis⁵⁰, A. Zacharopoulou⁵⁰, K. Adamidis⁵¹, I. Bestintzanos⁵¹, I. Evangelou⁵¹, C. Foudas⁵¹, P. Gianneios⁵¹, C. Kamtsikis⁵¹, P. Katsoulis⁵¹, P. Kokkas⁵¹, P. G. Kosmoglou Kioseoglou⁵¹, N. Manthos⁵¹, I. Papadopoulos⁵¹, J. Strologas⁵¹, M. Bartók^{52,ii}, C. Hajdu⁵², D. Horvath^{52,ji,kk}, F. Sikler⁵², V. Veszpremi⁵², M. Csanád⁵³, K. Farkas⁵³, M. M. A. Gadallah^{53,ii}, Á. Kadlecik⁵³, P. Major⁵³, K. Mandal⁵³, G. Pásztor⁵³, A. J. Rádl^{53,mmm}, G. I. Veres⁵³, P. Raics⁵⁴, B. Ujvari^{54,nn}, G. Zilizi⁵⁴, G. Bencze⁵⁵, S. Czellar⁵⁵, J. Karancsi^{55,ii}, J. Molnar⁵⁵, Z. Szillasi⁵⁵, T. Csorgo^{56,mmm}, F. Nemes^{56,mmm}, T. Novak⁵⁶, J. Babbar⁵⁷, S. Bansal⁵⁷, S. B. Beri⁵⁷, V. Bhatnagar⁵⁷, G. Chaudhary⁵⁷, S. Chauhan⁵⁷, N. Dhingra^{57,oo}, A. Kaur⁵⁷, A. Kaur⁵⁷, H. Kaur⁵⁷, M. Kaur⁵⁷, S. Kumar⁵⁷, M. Meena⁵⁷, K. Sandeep⁵⁷, T. Sheokand⁵⁷, J. B. Singh⁵⁷, A. Singla⁵⁷, A. Ahmed⁵⁸, A. Bhardwaj⁵⁸, A. Chhetri⁵⁸, B. C. Choudhary⁵⁸, A. Kumar⁵⁸, M. Naimuddin⁵⁸, K. Ranjan⁵⁸, S. Saumya⁵⁸, S. Acharya^{59,pp}, S. Baradia⁵⁹, S. Barman^{59,qq}, S. Bhattacharya⁵⁹, D. Bhowmik⁵⁹, S. Dutta⁵⁹, S. Dutta⁵⁹, P. Palit⁵⁹, B. Sahu^{59,pp}, S. Sarkar⁵⁹, M. M. Ameen⁶⁰, P. K. Behera⁶⁰, S. C. Behera⁶⁰, S. Chatterjee⁶⁰, P. Jana⁶⁰, P. Kalbhor⁶⁰, J. R. Komaragiri^{60,rr}, D. Kumar^{60,rr}, L. Panwar^{60,rr}, R. Pradhan⁶⁰, P. R. Pujahari⁶⁰, N. R. Saha⁶⁰, A. Sharma⁶⁰, A. K. Sikdar⁶⁰, S. Verma⁶⁰, T. Aziz⁶¹, I. Das⁶¹, S. Dugad⁶¹, M. Kumar⁶¹, G. B. Mohanty⁶¹, P. Suryadevara⁶¹, A. Bala⁶², S. Banerjee⁶², R. M. Chatterjee⁶², M. Guchait⁶², Sh. Jain⁶², S. Karmakar⁶², S. Kumar⁶², G. Majumder⁶², K. Mazumdar⁶², S. Mukherjee⁶², S. Parolia⁶², A. Thachayath⁶², S. Bahinipati^{63,ss}, A. K. Das⁶³, C. Kar⁶³, D. Maity^{63,tt}, P. Mal⁶³, T. Mishra⁶³, V. K. Muraleedharan Nair Bindhu^{63,tt}, K. Naskar^{63,tt}, A. Nayak^{63,tt}, P. Sadangi⁶³, P. Saha⁶³, S. K. Swain⁶³, S. Varghese^{63,tt}, D. Vats^{63,tt}, A. Alpana⁶⁴, S. Dube⁶⁴, B. Gomber^{64,pp}, B. Kansal⁶⁴, A. Laha⁶⁴, A. Rastogi⁶⁴, S. Sharma⁶⁴, H. Bakhshiansohi^{65,uu}, E. Khazaie^{65,vv}, M. Zeinali^{65,ww}, S. Chenarani^{66,xx}, A. Dokhani^{66,dd}, S. M. Etesami⁶⁶, G. Haghghat⁶⁶, M. Khakzad⁶⁶, M. Mohammadi Najafabadi⁶⁶, M. Grunewald⁶⁷, M. Abbrescia^{68a,68b}, R. Aly^{68a,68c,r}, A. Colaleo^{68a,68b}, D. Creanza^{68a,68c}, B. D'Anzi^{68a,68b}, N. De Filippis^{68a,68c}, M. De Palma^{68a,68b}, A. Di Florio^{68a,68c}, W. Elmetenawee^{68a,68b,r}, L. Fiore^{68a}, G. Iaselli^{68a,68c}, M. Louka^{68a,68b}, G. Maggi^{68a,68c}, M. Maggi^{68a}, I. Margjeka^{68a,68b}, V. Mastrapasqua^{68a,68b}, S. My^{68a,68b}, S. Nuzzo^{68a,68b}, A. Pellecchia^{68a,68b}, A. Pompili^{68a,68b}, G. Pugliese^{68a,68c}, R. Radogna^{68a}, G. Ramirez-Sanchez^{68a,68c}, D. Ramos^{68a}, A. Ranieri^{68a}, L. Silvestris^{68a}, F. M. Simone^{68a,68b}, Ü. Sözbilir^{68a}, A. Stamerra^{68a}, R. Venditti^{68a}, P. Verwilligen^{68a}, A. Zaza^{68a,68b}, G. Abbiendi^{69a}, C. Battilana^{69a,69b}, D. Bonacorsi^{69a,69b}, L. Borgonovi^{69a}, R. Campanini^{69a,69b}, P. Capiluppi^{69a,69b}, A. Castro^{69a,69b}, F. R. Cavallo^{69a}, M. Cuffiani^{69a,69b}, G. M. Dallavalle^{69a}, T. Diotallevi^{69a,69b}, F. Fabbri^{69a}, A. Fanfani^{69a,69b}, D. Fasanella^{69a,69b}, P. Giacomelli^{69a}, L. Giommi^{69a,69b}, C. Grandi^{69a}, L. Guiducci^{69a,69b}, S. Lo Meo^{69a,yy}, L. Lunerti^{69a,69b}, S. Marcellini^{69a}, G. Masetti^{69a}, F. L. Navarria^{69a,69b}, F. Primavera^{69a,69b}, A. M. Rossi^{69a,69b}, T. Rovelli^{69a,69b}, G. P. Siroli^{69a,69b}, S. Costa^{70a,70b,zz}, A. Di Mattia^{70a}, R. Potenza^{70a,70b}, A. Tricomi^{70a,70b,zz}, C. Tuve^{70a,70b}, G. Barbagli^{71a}, G. Bardelli^{71a,71b}, B. Camaiani^{71a,71b}, A. Cassese^{71a}, R. Ceccarelli^{71a}, V. Ciulli^{71a,71b}, C. Civinini^{71a}, R. D'Alessandro^{71a,71b}, E. Focardi^{71a,71b}, T. Kello^{71a}, G. Latino^{71a,71b}, P. Lenzi^{71a,71b}, M. Lizzo^{71a}, M. Meschini^{71a}, S. Paoletti^{71a}, A. Papanastassiou^{71a,71b}, G. Sguazzoni^{71a}, L. Viliani^{71a}, L. Benussi⁷², S. Bianco⁷², S. Meola^{72,aaa}, D. Piccolo⁷², P. Chatagnon^{73a}, F. Ferro^{73a}, E. Robutti^{73a}, S. Tosi^{73a,73b}, A. Benaglia^{74a}, G. Boldrini^{74a,74b}, F. Brivio^{74a}, F. Ceteorelli^{74a}, F. De Guio^{74a,74b}, M. E. Dinardo^{74a,74b}, P. Dini^{74a}, S. Gennai^{74a}, R. Gerosa^{74a,74b}, A. Ghezzi^{74a,74b}, P. Govoni^{74a,74b}, L. Guzzi^{74a}, M. T. Lucchini^{74a,74b}, M. Malberti^{74a}, S. Malvezzi^{74a}, A. Massironi^{74a}, D. Menasce^{74a}, L. Moroni^{74a}, M. Paganoni^{74a,74b}, D. Pedrini^{74a}, B. S. Pinolini^{74a}, S. Ragazzi^{74a,74b}, T. Tabarelli de Fatis^{74a,74b}, D. Zuolo^{74a}, S. Buontempo^{75a}, A. Cagnotta^{75a,75b}, F. Carnevali^{75a,75b}, N. Cavallo^{75a,75c}, A. De Iorio^{75a,75b}, F. Fabozzi^{75a,75c}, A. O. M. Iorio^{75a,75b}, L. Lista^{75a,75b,bbb}, P. Paolucci^{75a,hh}, B. Rossi^{75a}, C. Sciacca^{75a,75b}, R. Ardino^{76a}, P. Azzi^{76a}, N. Bacchetta^{76a,ccc}, D. Bisello^{76a,76b}, P. Bortignon^{76a}, A. Bragagnolo^{76a,76b}, R. Carlin^{76a,76b}, P. Checchia^{76a}, T. Dorigo^{76a}, F. Gasparini^{76a,76b}, U. Gasparini^{76a,76b}, G. Grosso^{76a}, L. Layer^{76a,ddd}, E. Lusiani^{76a}, M. Margoni^{76a,76b}, A. T. Meneguzzo^{76a,76b}, M. Migliorini^{76a,76b}, M. Passaseo^{76a}, J. Pazzini^{76a,76b}, P. Ronchese^{76a,76b}, R. Rossin^{76a,76b}, M. Sgaravatto^{76a}, F. Simonetto^{76a,76b}

G. Strong^{76a}, M. Tosi^{76a,76b}, A. Triossi^{76a,76b}, S. Ventura^{76a}, H. Yasar^{76a,76b}, P. Zotto^{76a,76b}, A. Zuchetta^{76a,76b}, S. Abu Zeid^{77a,u}, C. Aimè^{77a,77b}, A. Braghieri^{77a}, S. Calzaferri^{77a,77b}, D. Fiorina^{77a,77b}, P. Montagna^{77a,77b}, V. Re^{77a}, C. Riccardi^{77a,77b}, P. Salvini^{77a}, I. Vai^{77a,77b}, P. Vitulo^{77a,77b}, S. Ajmal^{78a,78b}, P. Asenov^{78a,eee}, G. M. Bilei^{78a}, D. Ciangottini^{78a,78b}, L. Fanò^{78a,78b}, M. Magherini^{78a,78b}, G. Mantovani^{78a,78b}, V. Mariani^{78a,78b}, M. Menichelli^{78a}, F. Moscatelli^{78a,eee}, A. Rossi^{78a,78b}, A. Santocchia^{78a,78b}, D. Spiga^{78a}, T. Tedeschi^{78a,78b}, P. Azzurri^{79a}, G. Bagliesi^{79a}, R. Bhattacharya^{79a}, L. Bianchini^{79a,79b}, T. Boccali^{79a}, E. Bossini^{79a}, D. Bruschini^{79a,79c}, R. Castaldi^{79a}, M. A. Ciocci^{79a,79b}, M. Cipriani^{79a,79b}, V. D'Amante^{79a,79d}, R. Dell'Orso^{79a}, S. Donato^{79a}, A. Giassi^{79a}, F. Ligabue^{79a,79c}, D. Matos Figueiredo^{79a}, A. Messineo^{79a,79b}, M. Musich^{79a,79b}, F. Palla^{79a}, A. Rizzi^{79a,79b}, G. Rolandi^{79a,79c}, S. Roy Chowdhury^{79a}, T. Sarkar^{79a}, A. Scribano^{79a}, P. Spagnolo^{79a}, R. Tenchini^{79a}, G. Tonelli^{79a,79b}, N. Turini^{79a,79d}, A. Venturi^{79a}, P. G. Verdini^{79a}, P. Barria^{80a}, M. Campana^{80a,80b}, F. Cavallari^{80a}, L. Cunqueiro Mendez^{80a,80b}, D. Del Re^{80a,80b}, E. Di Marco^{80a}, M. Diemoz^{80a}, F. Errico^{80a,80b}, E. Longo^{80a,80b}, P. Meridiani^{80a}, J. Mijuskovic^{80a,80b}, G. Organtini^{80a,80b}, F. Pandolfi^{80a}, R. Paramatti^{80a,80b}, C. Quaranta^{80a,80b}, S. Rahatlou^{80a,80b}, C. Rovelli^{80a}, F. Santanastasio^{80a,80b}, L. Soffi^{80a}, N. Amapane^{81a,81b}, R. Arcidiacono^{81a,81c}, S. Argiro^{81a,81b}, M. Arneodo^{81a,81c}, N. Bartosik^{81a}, R. Bellan^{81a,81b}, A. Bellora^{81a,81b}, C. Biino^{81a}, N. Cartiglia^{81a}, M. Costa^{81a,81b}, R. Covarelli^{81a,81b}, N. Demaria^{81a}, L. Finco^{81a}, M. Grippo^{81a,81b}, B. Kiani^{81a,81b}, F. Legger^{81a}, F. Luongo^{81a,81b}, C. Mariotti^{81a}, S. Maselli^{81a}, A. Mecca^{81a,81b}, E. Migliore^{81a,81b}, M. Monteno^{81a}, R. Mulargia^{81a}, M. M. Obertino^{81a,81b}, G. Ortona^{81a}, L. Pacher^{81a,81b}, N. Pastrone^{81a}, M. Pelliccioni^{81a}, M. Ruspa^{81a,81c}, F. Siviero^{81a,81b}, V. Sola^{81a,81b}, A. Solano^{81a,81b}, D. Soldi^{81a,81b}, A. Staiano^{81a}, C. Tarricone^{81a,81b}, D. Trocino^{81a}, G. Umoret^{81a,81b}, E. Vlasov^{81a,81b}, S. Belforte^{82a}, V. Candelise^{82a,82b}, M. Casarsa^{82a}, F. Cossutti^{82a}, K. De Leo^{82a,82b}, G. Della Ricca^{82a,82b}, S. Dogra⁸³, J. Hong⁸³, C. Huh⁸³, B. Kim⁸³, D. H. Kim⁸³, J. Kim⁸³, H. Lee⁸³, S. W. Lee⁸³, C. S. Moon⁸³, Y. D. Oh⁸³, M. S. Ryu⁸³, S. Sekmen⁸³, Y. C. Yang⁸³, M. S. Kim⁸⁴, G. Bak⁸⁵, P. Gwak⁸⁵, H. Kim⁸⁵, D. H. Moon⁸⁵, E. Asilar⁸⁶, D. Kim⁸⁶, T. J. Kim⁸⁶, J. A. Merlin⁸⁶, S. Choi⁸⁷, S. Han⁸⁷, B. Hong⁸⁷, K. Lee⁸⁷, K. S. Lee⁸⁷, S. Lee⁸⁷, J. Park⁸⁷, S. K. Park⁸⁷, J. Yoo⁸⁷, J. Goh⁸⁸, H. S. Kim⁸⁹, Y. Kim⁸⁹, S. Lee⁸⁹, J. Almond⁹⁰, J. H. Bhyun⁹⁰, J. Choi⁹⁰, W. Jun⁹⁰, J. Kim⁹⁰, J. S. Kim⁹⁰, S. Ko⁹⁰, H. Kwon⁹⁰, H. Lee⁹⁰, J. Lee⁹⁰, J. Lee⁹⁰, B. H. Oh⁹⁰, S. B. Oh⁹⁰, H. Seo⁹⁰, U. K. Yang⁹⁰, I. Yoon⁹⁰, W. Jang⁹¹, D. Y. Kang⁹¹, Y. Kang⁹¹, S. Kim⁹¹, B. Ko⁹¹, J. S. H. Lee⁹¹, Y. Lee⁹¹, I. C. Park⁹¹, Y. Roh⁹¹, I. J. Watson⁹¹, S. Yang⁹¹, S. Ha⁹², H. D. Yoo⁹², M. Choi⁹³, M. R. Kim⁹³, H. Lee⁹³, Y. Lee⁹³, I. Yu⁹³, T. Beyrouthy⁹⁴, Y. Maghrbi⁹⁴, K. Dreimanis⁹⁵, A. Gaile⁹⁵, G. Pikurs⁹⁵, A. Potrebko⁹⁵, M. Seidel⁹⁵, V. Veckalns^{95,fff}, N. R. Strautnieks⁹⁶, M. Ambrozas⁹⁷, A. Juodagalvis⁹⁷, A. Rinkevicius⁹⁷, G. Tamulaitis⁹⁷, N. Bin Norjoharuddeen⁹⁸, I. Yusuff^{98,ggg}, Z. Zolkapli⁹⁸, J. F. Benitez⁹⁹, A. Castaneda Hernandez⁹⁹, H. A. Encinas Acosta⁹⁹, L. G. Gallegos Maríñez⁹⁹, M. León Coello⁹⁹, J. A. Murillo Quijada⁹⁹, A. Sehrawat⁹⁹, L. Valencia Palomo⁹⁹, G. Ayala¹⁰⁰, H. Castilla-Valdez¹⁰⁰, E. De La Cruz-Burelo¹⁰⁰, I. Heredia-De La Cruz^{100,hhh}, R. Lopez-Fernandez¹⁰⁰, C. A. Mondragon Herrera¹⁰⁰, A. Sánchez Hernández¹⁰⁰, C. Oropeza Barrera¹⁰¹, M. Ramírez García¹⁰¹, I. Bautista¹⁰², I. Pedraza¹⁰², H. A. Salazar Ibarguen¹⁰², C. Uribe Estrada¹⁰², I. Bujanja¹⁰³, N. Raicevic¹⁰³, P. H. Butler¹⁰⁴, A. Ahmad¹⁰⁵, M. I. Asghar¹⁰⁵, A. Awais¹⁰⁵, M. I. M. Awan¹⁰⁵, H. R. Hoorani¹⁰⁵, W. A. Khan¹⁰⁵, V. Avati¹⁰⁶, L. Grzanka¹⁰⁶, M. Malawski¹⁰⁶, H. Bialkowska¹⁰⁷, M. Bluj¹⁰⁷, B. Boimska¹⁰⁷, M. Górski¹⁰⁷, M. Kazana¹⁰⁷, M. Szeleper¹⁰⁷, P. Zalewski¹⁰⁷, K. Bunkowski¹⁰⁸, K. Doroba¹⁰⁸, A. Kalinowski¹⁰⁸, M. Konecki¹⁰⁸, J. Krolikowski¹⁰⁸, A. Muhammad¹⁰⁸, K. Pozniak¹⁰⁹, W. Zabolotny¹⁰⁹, M. Araujo¹¹⁰, D. Bastos¹¹⁰, C. Beirão Da Cruz E Silva¹¹⁰, A. Boletti¹¹⁰, M. Bozzo¹¹⁰, T. Camporesi¹¹⁰, G. Da Molin¹¹⁰, P. Faccioli¹¹⁰, M. Gallinaro¹¹⁰, J. Hollar¹¹⁰, N. Leonardo¹¹⁰, T. Niknejad¹¹⁰, A. Petrilli¹¹⁰, M. Pisano¹¹⁰, J. Seixas¹¹⁰, J. Varela¹¹⁰, J. W. Wulff¹¹⁰, P. Adzic¹¹¹, P. Milenovic¹¹¹, M. Dordevic¹¹², J. Milosevic¹¹², V. Rekovic¹¹², M. Aguilar-Benitez¹¹³, J. Alcaraz Maestre¹¹³, Cristina F. Bedoya¹¹³, M. Cepeda¹¹³, M. Cerrada¹¹³, N. Colino¹¹³, B. De La Cruz¹¹³, A. Delgado Peris¹¹³, D. Fernández Del Val¹¹³, J. P. Fernández Ramos¹¹³, J. Flix¹¹³, M. C. Fouz¹¹³, O. Gonzalez Lopez¹¹³, S. Goy Lopez¹¹³, J. M. Hernandez¹¹³, M. I. Josa¹¹³, J. León Holgado¹¹³, D. Moran¹¹³, C. M. Morcillo Perez¹¹³, Á. Navarro Tobar¹¹³, C. Perez Dengra¹¹³, A. Pérez-Calero Yzquierdo¹¹³, J. Puerta Pelayo¹¹³, I. Redondo¹¹³, D. D. Redondo Ferrero¹¹³, L. Romero¹¹³, S. Sánchez Navas¹¹³, L. Urda Gómez¹¹³, J. Vazquez Escobar¹¹³, C. Willmott¹¹³, J. F. de Trocóniz¹¹⁴, B. Alvarez Gonzalez¹¹⁵, J. Cuevas¹¹⁵, J. Fernandez Menendez¹¹⁵, S. Folgueras¹¹⁵, I. Gonzalez Caballero¹¹⁵, J. R. González Fernández¹¹⁵, E. Palencia Cortezon¹¹⁵, C. Ramón Álvarez¹¹⁵, V. Rodríguez Bouza¹¹⁵

- A. Soto Rodríguez¹¹⁵, A. Trapote¹¹⁵, C. Vico Villalba¹¹⁵, P. Vischia¹¹⁵, S. Bhowmik¹¹⁶, S. Blanco Fernández¹¹⁶, J. A. Brochero Cifuentes¹¹⁶, I. J. Cabrillo¹¹⁶, A. Calderon¹¹⁶, J. Duarte Campderros¹¹⁶, M. Fernandez¹¹⁶, C. Fernandez Madrazo¹¹⁶, G. Gomez¹¹⁶, C. Lasasoa García¹¹⁶, C. Martinez Rivero¹¹⁶
- P. Martinez Ruiz del Arbol¹¹⁶, F. Matorras¹¹⁶, P. Matorras Cuevas¹¹⁶, E. Navarrete Ramos¹¹⁶, J. Piedra Gomez¹¹⁶, L. Scodellaro¹¹⁶, I. Vila¹¹⁶, J. M. Vizan Garcia¹¹⁶, M. K. Jayananda¹¹⁷, B. Kailasapathy^{117,iii}, D. U. J. Sonnadara¹¹⁷, D. D. C. Wickramaratna¹¹⁷, W. G. D. Dharmaratna^{118,iii}, K. Liyanage¹¹⁸, N. Perera¹¹⁸, N. Wickramage¹¹⁸, D. Abbaneo¹¹⁹, C. Amendola¹¹⁹, E. Auffray¹¹⁹, G. Auzinger¹¹⁹, J. Baechler¹¹⁹, D. Barney¹¹⁹, A. Bermúdez Martínez¹¹⁹, M. Bianco¹¹⁹, B. Bilin¹¹⁹, A. A. Bin Anuar¹¹⁹, A. Bocci¹¹⁹, E. Brondolin¹¹⁹, C. Caillol¹¹⁹, G. Cerminara¹¹⁹, N. Chernyavskaya¹¹⁹, D. d'Enterria¹¹⁹, A. Dabrowski¹¹⁹, A. David¹¹⁹, A. De Roeck¹¹⁹, M. M. Defranchis¹¹⁹, M. Deile¹¹⁹, M. Dobson¹¹⁹, F. Fallavollita^{119,kkk}, L. Forthomme¹¹⁹, G. Franzoni¹¹⁹, W. Funk¹¹⁹, S. Giani¹¹⁹, D. Gigi¹¹⁹, K. Gill¹¹⁹, F. Glege¹¹⁹, L. Gouskos¹¹⁹, M. Haranko¹¹⁹, J. Hegeman¹¹⁹, B. Huber¹¹⁹, V. Innocente¹¹⁹, T. James¹¹⁹, P. Janot¹¹⁹, S. Laurila¹¹⁹, P. Lecoq¹¹⁹, E. Leutgeb¹¹⁹, C. Lourenço¹¹⁹, B. Maier¹¹⁹, L. Malgeri¹¹⁹, M. Mannelli¹¹⁹, A. C. Marini¹¹⁹, M. Matthewman¹¹⁹, F. Meijers¹¹⁹, S. Mersi¹¹⁹, E. Meschi¹¹⁹, V. Milosevic¹¹⁹, F. Moortgat¹¹⁹, M. Mulders¹¹⁹, S. Orfanelli¹¹⁹, F. Pantaleo¹¹⁹, G. Petrucciani¹¹⁹, A. Pfeiffer¹¹⁹, M. Pierini¹¹⁹, D. Piparo¹¹⁹, H. Qu¹¹⁹, D. Rabady¹¹⁹, G. Reales Gutiérrez¹¹⁹, M. Rovere¹¹⁹, H. Sakulin¹¹⁹, S. Scarfi¹¹⁹, C. Schwick¹¹⁹, M. Selvaggi¹¹⁹, A. Sharma¹¹⁹, K. Shchelina¹¹⁹, P. Silva¹¹⁹, P. Sphicas^{119,iii}, A. G. Stahl Leiton¹¹⁹, A. Steen¹¹⁹, S. Summers¹¹⁹, D. Treille¹¹⁹, P. Tropea¹¹⁹, A. Tsiros¹¹⁹, D. Walter¹¹⁹, J. Wanczyk^{119,mmm}, K. A. Wozniak^{119,nnn}, S. Wuchterl¹¹⁹, P. Zehetner¹¹⁹, P. Zexid¹¹⁹, W. D. Zeuner¹¹⁹, T. Bevilacqua^{120,ooo}, L. Caminada^{120,ooo}, A. Ebrahimi¹²⁰, W. Erdmann¹²⁰, R. Horisberger¹²⁰, Q. Ingram¹²⁰, H. C. Kaestli¹²⁰, D. Kotlinski¹²⁰, C. Lange¹²⁰, M. Missiroli^{120,ooo}, L. Nohte^{120,ooo}, T. Rohe¹²⁰, T. K. Aarrestad¹²¹, K. Androsov^{121,mmm}, M. Backhaus¹²¹, A. Calandri¹²¹, C. Cazzaniga¹²¹, K. Datta¹²¹, A. De Cosa¹²¹, G. Dissertori¹²¹, M. Dittmar¹²¹, M. Donegà¹²¹, F. Eble¹²¹, M. Galli¹²¹, K. Gedia¹²¹, F. Glessgen¹²¹, C. Grab¹²¹, D. Hits¹²¹, W. Lustermann¹²¹, A.-M. Lyon¹²¹, R. A. Manzoni¹²¹, M. Marchegiani¹²¹, L. Marchese¹²¹, C. Martin Perez¹²¹, A. Mascellani^{121,mmm}, F. Nessi-Tedaldi¹²¹, F. Pauss¹²¹, V. Perovic¹²¹, S. Pigazzini¹²¹, M. G. Ratti¹²¹, M. Reichmann¹²¹, C. Reissel¹²¹, T. Reitenspiess¹²¹, B. Ristic¹²¹, F. Riti¹²¹, D. Ruini¹²¹, D. A. Sanz Becerra¹²¹, R. Seidita¹²¹, J. Steggemann^{121,mmm}, D. Valsecchi¹²¹, R. Wallny¹²¹, C. AMSLER^{122,ppp}, P. Bäertschi¹²², C. Botta¹²², D. Brzhechko¹²², M. F. Canelli¹²², K. Cormier¹²², R. Del Burgo¹²², J. K. Heikkilä¹²², M. Huwiler¹²², W. Jin¹²², A. Jofrehei¹²², B. Kilminster¹²², S. Leontsinis¹²², S. P. Liechi¹²², A. Macchiolo¹²², P. Meiring¹²², V. M. Mikuni¹²², U. Molinatti¹²², I. Neutelings¹²², A. Reimers¹²², P. Robmann¹²², S. Sanchez Cruz¹²², K. Schweiger¹²², M. Senger¹²², Y. Takahashi¹²², R. Tramontano¹²², C. Adloff^{123,qqq}, C. M. Kuo¹²³, W. Lin¹²³, P. K. Rout¹²³, P. C. Tiwari^{123,rr}, S. S. Yu¹²³, L. Ceard¹²⁴, Y. Chao¹²⁴, K. F. Chen¹²⁴, P. s. Chen¹²⁴, Z. g. Chen¹²⁴, W.-S. Hou¹²⁴, T. h. Hsu¹²⁴, Y. w. Kao¹²⁴, R. Khurana¹²⁴, G. Kole¹²⁴, Y. y. Li¹²⁴, R.-S. Lu¹²⁴, E. Paganis¹²⁴, A. Psallidas¹²⁴, X. f. Su¹²⁴, J. Thomas-Wilsker¹²⁴, L. s. Tsai¹²⁴, H. y. Wu¹²⁴, E. Yazgan¹²⁴, C. Asawatangkuldee¹²⁵, N. Srimanobhas¹²⁵, V. Wachirapusanand¹²⁵, D. Agyel¹²⁶, F. Boran¹²⁶, Z. S. Demiroglu¹²⁶, F. Dolek¹²⁶, I. Dumanoglu^{126,rrr}, E. Eskut¹²⁶, Y. Guler^{126,sss}, E. Gurpinar Guler^{126,sss}, C. Isik¹²⁶, O. Kara¹²⁶, A. Kayis Topaksu¹²⁶, U. Kiminsu¹²⁶, G. Onengut¹²⁶, K. Ozdemir^{126,ttt}, A. Polatoz¹²⁶, B. Tali^{126,uuu}, U. G. Tok¹²⁶, S. Turkcapar¹²⁶, E. Uslan¹²⁶, I. S. Zorbakir¹²⁶, M. Yalvac^{127,vvv}, B. Akgun¹²⁸, I. O. Atakisi¹²⁸, E. Gülmez¹²⁸, M. Kaya^{128,www}, O. Kaya^{128,xxx}, S. Tekten^{128,yyy}, A. Cakir¹²⁹, K. Cankocak^{129,rrr,zzz}, Y. Komurcu¹²⁹, S. Sen^{129,aaaa}, O. Aydilek¹³⁰, S. Cerci^{130,uuu}, V. Epshteyn¹³⁰, B. Haciasahinoglu¹³⁰, I. Hos^{130,bbbb}, B. Isildak^{130,cccc}, B. Kaynak¹³⁰, S. Ozkorucuklu¹³⁰, O. Potok¹³⁰, H. Sert¹³⁰, C. Simsek¹³⁰, D. Sunar Cerci^{130,uuu}, C. Zorbilmez¹³⁰, A. Boyaryntsev¹³¹, B. Grynyov¹³¹, L. Levchuk¹³², D. Anthony¹³³, J. J. Brooke¹³³, A. Bundock¹³³, F. Bury¹³³, E. Clement¹³³, D. Cussans¹³³, H. Flacher¹³³, M. Glowacki¹³³, J. Goldstein¹³³, H. F. Heath¹³³, L. Kreczko¹³³, B. Krikler¹³³, S. Paramesvaran¹³³, S. Seif El Nasr-Storey¹³³, V. J. Smith¹³³, N. Stylianou^{133,dddd}, K. Walkingshaw Pass¹³³, R. White¹³³, A. H. Ball¹³⁴, K. W. Bell¹³⁴, A. Belyaev^{134,eeee}, C. Brew¹³⁴, R. M. Brown¹³⁴, D. J. A. Cockerill¹³⁴, C. Cooke¹³⁴, K. V. Ellis¹³⁴, K. Harder¹³⁴, S. Harper¹³⁴, M.-L. Holmberg^{134,ffff}, J. Linacre¹³⁴, K. Manolopoulos¹³⁴, D. M. Newbold¹³⁴, E. Olaiya¹³⁴, D. Petyt¹³⁴, T. Reis¹³⁴, G. Salvi¹³⁴, T. Schuh¹³⁴, C. H. Shepherd-Themistocleous¹³⁴, I. R. Tomalin¹³⁴, T. Williams¹³⁴, R. Bainbridge¹³⁵, P. Bloch¹³⁵, C. E. Brown¹³⁵, O. Buchmuller¹³⁵, V. Cacchio¹³⁵, C. A. Carrillo Montoya¹³⁵, G. S. Chahal^{135,gggg}, D. Colling¹³⁵, J. S. Dancu¹³⁵, P. Dauncey¹³⁵, G. Davies¹³⁵

J. Davies,¹³⁵ M. Della Negra,¹³⁵ S. Fayer,¹³⁵ G. Fedi,¹³⁵ G. Hall,¹³⁵ M. H. Hassanshahi,¹³⁵ A. Howard,¹³⁵ G. Iles,¹³⁵ M. Knight,¹³⁵ J. Langford,¹³⁵ L. Lyons,¹³⁵ A.-M. Magnan,¹³⁵ S. Malik,¹³⁵ A. Martelli,¹³⁵ M. Mieskolainen,¹³⁵ J. Nash,^{135,hhhh} M. Pesaresi,¹³⁵ B. C. Radburn-Smith,¹³⁵ A. Richards,¹³⁵ A. Rose,¹³⁵ C. Seez,¹³⁵ R. Shukla,¹³⁵ A. Tapper,¹³⁵ K. Uchida,¹³⁵ G. P. Uttley,¹³⁵ L. H. Vage,¹³⁵ T. Virdee,^{135,hh} M. Vojinovic,¹³⁵ N. Wardle,¹³⁵ D. Winterbottom,¹³⁵ K. Coldham,¹³⁶ J. E. Cole,¹³⁶ A. Khan,¹³⁶ P. Kyberd,¹³⁶ I. D. Reid,¹³⁶ S. Abdullin,¹³⁷ A. Brinkerhoff,¹³⁷ B. Caraway,¹³⁷ J. Dittmann,¹³⁷ K. Hatakeyama,¹³⁷ J. Hiltbrand,¹³⁷ A. R. Kanuganti,¹³⁷ B. McMaster,¹³⁷ M. Saunders,¹³⁷ S. Sawant,¹³⁷ C. Sutantawibul,¹³⁷ M. Toms,^{137,q} J. Wilson,¹³⁷ R. Bartek,¹³⁸ A. Dominguez,¹³⁸ C. Huerta Escamilla,¹³⁸ A. E. Simsek,¹³⁸ R. Uniyal,¹³⁸ A. M. Vargas Hernandez,¹³⁸ R. Chudasama,¹³⁹ S. I. Cooper,¹³⁹ S. V. Gleyzer,¹³⁹ C. U. Perez,¹³⁹ P. Rumerio,^{139,iiii} E. Usai,¹³⁹ C. West,¹³⁹ R. Yi,¹³⁹ A. Akpinar,¹⁴⁰ A. Albert,¹⁴⁰ D. Arcaro,¹⁴⁰ C. Cosby,¹⁴⁰ Z. Demiragli,¹⁴⁰ C. Erice,¹⁴⁰ E. Fontanesi,¹⁴⁰ D. Gastler,¹⁴⁰ S. Jeon,¹⁴⁰ J. Rohlf,¹⁴⁰ K. Salyer,¹⁴⁰ D. Sperka,¹⁴⁰ D. Spitzbart,¹⁴⁰ I. Suarez,¹⁴⁰ A. Tsatsos,¹⁴⁰ S. Yuan,¹⁴⁰ G. Benelli,¹⁴¹ X. Coubez,^{141,cc} D. Cutts,¹⁴¹ M. Hadley,¹⁴¹ U. Heintz,¹⁴¹ J. M. Hogan,^{141,jiii} T. Kwon,¹⁴¹ G. Landsberg,¹⁴¹ K. T. Lau,¹⁴¹ D. Li,¹⁴¹ J. Luo,¹⁴¹ S. Mondal,¹⁴¹ M. Narain,^{141,a} N. Pervan,¹⁴¹ S. Sagir,^{141,kkkk} F. Simpson,¹⁴¹ M. Stamenkovic,¹⁴¹ W. Y. Wong,¹⁴¹ X. Yan,¹⁴¹ W. Zhang,¹⁴¹ S. Abbott,¹⁴² J. Bonilla,¹⁴² C. Brainerd,¹⁴² R. Breedon,¹⁴² M. Calderon De La Barca Sanchez,¹⁴² M. Chertok,¹⁴² M. Citron,¹⁴² J. Conway,¹⁴² P. T. Cox,¹⁴² R. Erbacher,¹⁴² F. Jensen,¹⁴² O. Kukral,¹⁴² G. Mocellin,¹⁴² M. Mulhearn,¹⁴² D. Pellett,¹⁴² W. Wei,¹⁴² Y. Yao,¹⁴² F. Zhang,¹⁴² M. Bachtis,¹⁴³ R. Cousins,¹⁴³ A. Datta,¹⁴³ J. Hauser,¹⁴³ M. Ignatenko,¹⁴³ M. A. Iqbal,¹⁴³ T. Lam,¹⁴³ E. Manca,¹⁴³ D. Saltzberg,¹⁴³ V. Valuev,¹⁴³ R. Clare,¹⁴⁴ J. W. Gary,¹⁴⁴ M. Gordon,¹⁴⁴ G. Hanson,¹⁴⁴ W. Si,¹⁴⁴ S. Wimpenny,^{144,a} J. G. Branson,¹⁴⁵ S. Cittolin,¹⁴⁵ S. Cooperstein,¹⁴⁵ D. Diaz,¹⁴⁵ J. Duarte,¹⁴⁵ L. Giannini,¹⁴⁵ J. Guiang,¹⁴⁵ R. Kansal,¹⁴⁵ V. Krutelyov,¹⁴⁵ R. Lee,¹⁴⁵ J. Letts,¹⁴⁵ M. Masciovecchio,¹⁴⁵ F. Mokhtar,¹⁴⁵ M. Pieri,¹⁴⁵ M. Quinnan,¹⁴⁵ B. V. Sathia Narayanan,¹⁴⁵ V. Sharma,¹⁴⁵ M. Tadel,¹⁴⁵ E. Vourliotis,¹⁴⁵ F. Würthwein,¹⁴⁵ Y. Xiang,¹⁴⁵ A. Yagil,¹⁴⁵ A. Barzdukas,¹⁴⁶ L. Brennan,¹⁴⁶ C. Campagnari,¹⁴⁶ G. Collura,¹⁴⁶ A. Dorsett,¹⁴⁶ J. Incandela,¹⁴⁶ M. Kilpatrick,¹⁴⁶ J. Kim,¹⁴⁶ A. J. Li,¹⁴⁶ P. Masterson,¹⁴⁶ H. Mei,¹⁴⁶ M. Oshiro,¹⁴⁶ J. Richman,¹⁴⁶ U. Sarica,¹⁴⁶ R. Schmitz,¹⁴⁶ F. Setti,¹⁴⁶ J. Sheplock,¹⁴⁶ D. Stuart,¹⁴⁶ S. Wang,¹⁴⁶ A. Bornheim,¹⁴⁷ O. Cerri,¹⁴⁷ A. Latorre,¹⁴⁷ J. Mao,¹⁴⁷ H. B. Newman,¹⁴⁷ T. Q. Nguyen,¹⁴⁷ M. Spiropulu,¹⁴⁷ J. R. Vlimant,¹⁴⁷ C. Wang,¹⁴⁷ S. Xie,¹⁴⁷ R. Y. Zhu,¹⁴⁷ J. Alison,¹⁴⁸ S. An,¹⁴⁸ M. B. Andrews,¹⁴⁸ P. Bryant,¹⁴⁸ V. Dutta,¹⁴⁸ T. Ferguson,¹⁴⁸ A. Harilal,¹⁴⁸ C. Liu,¹⁴⁸ T. Mudholkar,¹⁴⁸ S. Murthy,¹⁴⁸ M. Paulini,¹⁴⁸ A. Roberts,¹⁴⁸ A. Sanchez,¹⁴⁸ W. Terrill,¹⁴⁸ J. P. Cumalat,¹⁴⁹ W. T. Ford,¹⁴⁹ A. Hassani,¹⁴⁹ G. Karathanasis,¹⁴⁹ E. MacDonald,¹⁴⁹ N. Manganelli,¹⁴⁹ F. Marini,¹⁴⁹ A. Perloff,¹⁴⁹ C. Savard,¹⁴⁹ N. Schonbeck,¹⁴⁹ K. Stenson,¹⁴⁹ K. A. Ulmer,¹⁴⁹ S. R. Wagner,¹⁴⁹ N. Zipper,¹⁴⁹ J. Alexander,¹⁵⁰ S. Bright-Thonney,¹⁵⁰ X. Chen,¹⁵⁰ D. J. Cranshaw,¹⁵⁰ J. Fan,¹⁵⁰ X. Fan,¹⁵⁰ D. Gadkari,¹⁵⁰ S. Hogan,¹⁵⁰ J. Monroy,¹⁵⁰ J. R. Patterson,¹⁵⁰ J. Reichert,¹⁵⁰ M. Reid,¹⁵⁰ A. Ryd,¹⁵⁰ J. Thom,¹⁵⁰ P. Wittich,¹⁵⁰ R. Zou,¹⁵⁰ M. Albrow,¹⁵¹ M. Alyari,¹⁵¹ O. Amram,¹⁵¹ G. Apollinari,¹⁵¹ A. Apresyan,¹⁵¹ L. A. T. Bauerdick,¹⁵¹ D. Berry,¹⁵¹ J. Berryhill,¹⁵¹ P. C. Bhat,¹⁵¹ K. Burkett,¹⁵¹ J. N. Butler,¹⁵¹ A. Canepa,¹⁵¹ G. B. Cerati,¹⁵¹ H. W. K. Cheung,¹⁵¹ F. Chlebana,¹⁵¹ G. Cummings,¹⁵¹ J. Dickinson,¹⁵¹ I. Dutta,¹⁵¹ V. D. Elvira,¹⁵¹ Y. Feng,¹⁵¹ J. Freeman,¹⁵¹ A. Gandrakota,¹⁵¹ Z. Geise,¹⁵¹ L. Gray,¹⁵¹ D. Green,¹⁵¹ A. Grummer,¹⁵¹ S. Grünendahl,¹⁵¹ D. Guerrero,¹⁵¹ O. Gutsche,¹⁵¹ R. M. Harris,¹⁵¹ R. Heller,¹⁵¹ T. C. Herwig,¹⁵¹ J. Hirschauer,¹⁵¹ L. Horyn,¹⁵¹ B. Jayatilaka,¹⁵¹ S. Jindariani,¹⁵¹ M. Johnson,¹⁵¹ U. Joshi,¹⁵¹ T. Klijnsma,¹⁵¹ B. Klima,¹⁵¹ K. H. M. Kwok,¹⁵¹ S. Lammel,¹⁵¹ D. Lincoln,¹⁵¹ R. Lipton,¹⁵¹ T. Liu,¹⁵¹ C. Madrid,¹⁵¹ K. Maeshima,¹⁵¹ C. Mantilla,¹⁵¹ D. Mason,¹⁵¹ P. McBride,¹⁵¹ P. Merkel,¹⁵¹ S. Mrenna,¹⁵¹ S. Nahn,¹⁵¹ J. Ngadiuba,¹⁵¹ D. Noonan,¹⁵¹ V. Papadimitriou,¹⁵¹ N. Pastika,¹⁵¹ K. Pedro,¹⁵¹ C. Pena,^{151,iiii} F. Ravera,¹⁵¹ A. Reinsvold Hall,^{151,mmmm} L. Ristori,¹⁵¹ E. Sexton-Kennedy,¹⁵¹ N. Smith,¹⁵¹ A. Soha,¹⁵¹ L. Spiegel,¹⁵¹ S. Stoynev,¹⁵¹ J. Strait,¹⁵¹ L. Taylor,¹⁵¹ S. Tkaczyk,¹⁵¹ N. V. Tran,¹⁵¹ L. Uplegger,¹⁵¹ E. W. Vaandering,¹⁵¹ I. Zoi,¹⁵¹ C. Aruta,¹⁵² P. Avery,¹⁵² D. Bourilkov,¹⁵² L. Cadamuro,¹⁵² P. Chang,¹⁵² V. Cherepanov,¹⁵² R. D. Field,¹⁵² E. Koenig,¹⁵² M. Kolosova,¹⁵² J. Konigsberg,¹⁵² A. Korytov,¹⁵² K. H. Lo,¹⁵² K. Matchev,¹⁵² N. Menendez,¹⁵² G. Mitselmakher,¹⁵² K. Mohrman,¹⁵² A. Muthirakalayil Madhu,¹⁵² N. Rawal,¹⁵² D. Rosenzweig,¹⁵² S. Rosenzweig,¹⁵² K. Shi,¹⁵² J. Wang,¹⁵² T. Adams,¹⁵³ A. Al Kadhimi,¹⁵³ A. Askew,¹⁵³ N. Bower,¹⁵³ R. Habibullah,¹⁵³ V. Hagopian,¹⁵³ R. Hashmi,¹⁵³ R. S. Kim,¹⁵³ S. Kim,¹⁵³ T. Kolberg,¹⁵³ G. Martinez,¹⁵³ H. Prosper,¹⁵³ P. R. Prova,¹⁵³ O. Viazlo,¹⁵³ M. Wulansatiti,¹⁵³ R. Yohay,¹⁵³ J. Zhang,¹⁵³

B. Alsufyani,¹⁵⁴ M. M. Baarmand¹⁵⁴ S. Butalla¹⁵⁴ T. Elkafrawy^{154,u} M. Hohlmann¹⁵⁴ R. Kumar Verma¹⁵⁴
 M. Rahmani,¹⁵⁴ M. R. Adams¹⁵⁵ C. Bennett,¹⁵⁵ R. Cavanaugh¹⁵⁵ S. Dittmer¹⁵⁵ R. Escobar Franco¹⁵⁵
 O. Evdokimov¹⁵⁵ C. E. Gerber¹⁵⁵ D. J. Hofman¹⁵⁵ J. h. Lee¹⁵⁵ D. S. Lemos¹⁵⁵ A. H. Merrit¹⁵⁵ C. Mills¹⁵⁵
 S. Nanda¹⁵⁵ G. Oh¹⁵⁵ B. Ozek¹⁵⁵ D. Pilipovic¹⁵⁵ T. Roy¹⁵⁵ S. Rudrabhatla¹⁵⁵ M. B. Tonjes¹⁵⁵
 N. Varelas¹⁵⁵ X. Wang¹⁵⁵ Z. Ye¹⁵⁵ J. Yoo¹⁵⁵ M. Alhousseini¹⁵⁶ D. Blend¹⁵⁶ K. Dilsiz^{156,nnnn} L. Emediato¹⁵⁶
 G. Karaman¹⁵⁶ O. K. Köseyan¹⁵⁶ J.-P. Merlo,¹⁵⁶ A. Mestvirishvili^{156,oooo} J. Nachtman¹⁵⁶ O. Neogi,¹⁵⁶
 H. Ogul^{156,pppp} Y. Onel¹⁵⁶ A. Penzo¹⁵⁶ C. Snyder,¹⁵⁶ E. Tiras^{156,qqqq} B. Blumenfeld¹⁵⁷ L. Corcodilos¹⁵⁷
 J. Davis¹⁵⁷ A. V. Gritsan¹⁵⁷ L. Kang¹⁵⁷ S. Kyriacou¹⁵⁷ P. Maksimovic¹⁵⁷ M. Roguljic¹⁵⁷ J. Roskes¹⁵⁷
 S. Sekhar¹⁵⁷ M. Swartz¹⁵⁷ T. Á. Vámi¹⁵⁷ A. Abreu¹⁵⁸ L. F. Alcerro Alcerro¹⁵⁸ J. Anguiano¹⁵⁸ P. Baringer¹⁵⁸
 A. Bean¹⁵⁸ Z. Flowers¹⁵⁸ D. Grove¹⁵⁸ J. King¹⁵⁸ G. Krintiras¹⁵⁸ M. Lazarovits¹⁵⁸ C. Le Mahieu¹⁵⁸
 C. Lindsey,¹⁵⁸ J. Marquez¹⁵⁸ N. Minafra¹⁵⁸ M. Murray¹⁵⁸ M. Nickel¹⁵⁸ M. Pitt¹⁵⁸ S. Popescu^{158,rrrr}
 C. Rogan¹⁵⁸ C. Royon¹⁵⁸ R. Salvatico¹⁵⁸ S. Sanders¹⁵⁸ C. Smith¹⁵⁸ Q. Wang¹⁵⁸ G. Wilson¹⁵⁸
 B. Allmond¹⁵⁹ A. Ivanov¹⁵⁹ K. Kaadze¹⁵⁹ A. Kalogeropoulos¹⁵⁹ D. Kim,¹⁵⁹ Y. Maravin¹⁵⁹ K. Nam,¹⁵⁹
 J. Natoli¹⁵⁹ D. Roy¹⁵⁹ G. Sorrentino¹⁵⁹ F. Rebassoo¹⁶⁰ D. Wright¹⁶⁰ A. Baden¹⁶¹ A. Belloni¹⁶¹
 A. Bethani¹⁶¹ Y. M. Chen¹⁶¹ S. C. Eno¹⁶¹ N. J. Hadley¹⁶¹ S. Jabeen¹⁶¹ R. G. Kellogg¹⁶¹ T. Koeth¹⁶¹
 Y. Lai¹⁶¹ S. Lascio¹⁶¹ A. C. Mignerey¹⁶¹ S. Nabili¹⁶¹ C. Palmer¹⁶¹ C. Papageorgakis¹⁶¹ M. M. Paranjpe,¹⁶¹
 L. Wang¹⁶¹ J. Bendavid¹⁶² W. Busza¹⁶² I. A. Cali¹⁶² Y. Chen¹⁶² M. D'Alfonso¹⁶² J. Eysermans¹⁶²
 C. Freer¹⁶² G. Gomez-Ceballos¹⁶² M. Goncharov,¹⁶² P. Harris,¹⁶² D. Hoang,¹⁶² D. Kovalskiy¹⁶² J. Krupa¹⁶²
 L. Lavezzo¹⁶² Y.-J. Lee¹⁶² K. Long¹⁶² C. Mironov¹⁶² C. Paus¹⁶² D. Rankin¹⁶² C. Roland¹⁶² G. Roland¹⁶²
 S. Rothman¹⁶² Z. Shi¹⁶² G. S. F. Stephans¹⁶² J. Wang,¹⁶² Z. Wang¹⁶² B. Wyslouch¹⁶² T. J. Yang¹⁶²
 B. Crossman¹⁶³ B. M. Joshi¹⁶³ C. Kapsiak¹⁶³ M. Krohn¹⁶³ D. Mahon¹⁶³ J. Mans¹⁶³ B. Marzocchi¹⁶³
 S. Pandey¹⁶³ M. Revering¹⁶³ R. Rusack¹⁶³ R. Saradhy¹⁶³ N. Schroeder¹⁶³ N. Strobbe¹⁶³ M. A. Wadud¹⁶³
 L. M. Cremaldi¹⁶⁴ K. Bloom¹⁶⁵ M. Bryson,¹⁶⁵ D. R. Claes¹⁶⁵ C. Fangmeier¹⁶⁵ F. Golf¹⁶⁵ G. Haza¹⁶⁵
 J. Hossain¹⁶⁵ C. Joo¹⁶⁵ I. Kravchenko¹⁶⁵ I. Reed¹⁶⁵ J. E. Siado¹⁶⁵ W. Tabb¹⁶⁵ A. Vagnerini¹⁶⁵
 A. Wightman¹⁶⁵ F. Yan¹⁶⁵ D. Yu¹⁶⁵ A. G. Zecchinelli¹⁶⁵ G. Agarwal¹⁶⁶ H. Bandyopadhyay¹⁶⁶ L. Hay¹⁶⁶
 I. Iashvili¹⁶⁶ A. Kharchilava¹⁶⁶ M. Morris¹⁶⁶ D. Nguyen¹⁶⁶ S. Rappoccio¹⁶⁶ H. Rejeb Sfar,¹⁶⁶ A. Williams¹⁶⁶
 E. Barberis¹⁶⁷ Y. Haddad¹⁶⁷ Y. Han¹⁶⁷ A. Krishna¹⁶⁷ J. Li¹⁶⁷ M. Lu¹⁶⁷ G. Madigan¹⁶⁷ R. Mccarthy¹⁶⁷
 D. M. Morse¹⁶⁷ V. Nguyen¹⁶⁷ T. Orimoto¹⁶⁷ A. Parker¹⁶⁷ L. Skinnari¹⁶⁷ A. Tishelman-Charny¹⁶⁷
 B. Wang¹⁶⁷ D. Wood¹⁶⁷ S. Bhattacharya¹⁶⁸ J. Bueghly,¹⁶⁸ Z. Chen¹⁶⁸ K. A. Hahn¹⁶⁸ Y. Liu¹⁶⁸ Y. Miao¹⁶⁸
 D. G. Monk¹⁶⁸ M. H. Schmitt¹⁶⁸ A. Taliervo¹⁶⁸ M. Velasco,¹⁶⁸ R. Band¹⁶⁹ R. Bucci,¹⁶⁹ S. Castells¹⁶⁹
 M. Cremonesi,¹⁶⁹ A. Das¹⁶⁹ R. Goldouzian¹⁶⁹ M. Hildreth¹⁶⁹ K. W. Ho¹⁶⁹ K. Hurtado Anampa¹⁶⁹ T. Ivanov¹⁶⁹
 C. Jessop¹⁶⁹ K. Lannon¹⁶⁹ J. Lawrence¹⁶⁹ N. Loukas¹⁶⁹ L. Lutton¹⁶⁹ J. Mariano,¹⁶⁹ N. Marinelli,¹⁶⁹
 I. Mcalister,¹⁶⁹ T. McCauley¹⁶⁹ C. Mcgrady¹⁶⁹ C. Moore¹⁶⁹ Y. Musienko^{169,q} H. Nelson¹⁶⁹ M. Osherson¹⁶⁹
 A. Piccinelli¹⁶⁹ R. Ruchti¹⁶⁹ A. Townsend¹⁶⁹ Y. Wan,¹⁶⁹ M. Wayne¹⁶⁹ H. Yockey,¹⁶⁹ M. Zarucki¹⁶⁹
 L. Zygala¹⁶⁹ A. Basnet¹⁷⁰ B. Bylsma,¹⁷⁰ M. Carrigan¹⁷⁰ L. S. Durkin¹⁷⁰ C. Hill¹⁷⁰ M. Joyce¹⁷⁰
 A. Lesauvage¹⁷⁰ M. Nunez Ornelas¹⁷⁰ K. Wei,¹⁷⁰ B. L. Winer¹⁷⁰ B. R. Yates¹⁷⁰ F. M. Addesa¹⁷¹
 H. Bouchamaoui¹⁷¹ P. Das¹⁷¹ G. Dezoort¹⁷¹ P. Elmer¹⁷¹ A. Frankenthal¹⁷¹ B. Greenberg¹⁷¹ N. Haubrich¹⁷¹
 S. Higginbotham¹⁷¹ G. Kopp¹⁷¹ S. Kwan¹⁷¹ D. Lange¹⁷¹ A. Loeliger¹⁷¹ D. Marlow¹⁷¹ I. Ojalvo¹⁷¹
 J. Olsen¹⁷¹ A. Shevelev¹⁷¹ D. Stickland¹⁷¹ C. Tully¹⁷¹ S. Malik¹⁷² A. S. Bakshi¹⁷³ V. E. Barnes¹⁷³
 S. Chandra¹⁷³ R. Chawla¹⁷³ S. Das¹⁷³ A. Gu¹⁷³ L. Gutay,¹⁷³ M. Jones¹⁷³ A. W. Jung¹⁷³ D. Kondratyev¹⁷³
 A. M. Koshy,¹⁷³ M. Liu¹⁷³ G. Negro¹⁷³ N. Neumeister¹⁷³ G. Paspalaki¹⁷³ S. Piperov¹⁷³ V. Scheurer,¹⁷³
 J. F. Schulte¹⁷³ M. Stojanovic¹⁷³ J. Thieman¹⁷³ A. K. Viridi¹⁷³ F. Wang¹⁷³ W. Xie¹⁷³ J. Dolen¹⁷⁴
 N. Parashar¹⁷⁴ A. Pathak¹⁷⁴ D. Acosta¹⁷⁵ A. Baty¹⁷⁵ T. Carnahan¹⁷⁵ K. M. Ecklund¹⁷⁵
 P. J. Fernández Manteca¹⁷⁵ S. Freed,¹⁷⁵ P. Gardner,¹⁷⁵ F. J. M. Geurts¹⁷⁵ A. Kumar¹⁷⁵ W. Li¹⁷⁵
 O. Miguel Colin¹⁷⁵ B. P. Padley¹⁷⁵ R. Redjimi,¹⁷⁵ J. Rotter¹⁷⁵ E. Yigitbasi¹⁷⁵ Y. Zhang¹⁷⁵ A. Bodek¹⁷⁶
 P. de Barbaro¹⁷⁶ R. Demina¹⁷⁶ J. L. Dulemba¹⁷⁶ C. Fallon,¹⁷⁶ A. Garcia-Bellido¹⁷⁶ O. Hindrichs¹⁷⁶
 A. Khukhunaishvili¹⁷⁶ P. Parygin^{176,q} E. Popova^{176,q} R. Taus¹⁷⁶ G. P. Van Onsem¹⁷⁶ K. Goulianos¹⁷⁷
 B. Chiarito,¹⁷⁸ J. P. Chou¹⁷⁸ Y. Gershtein¹⁷⁸ E. Halkiadakis¹⁷⁸ A. Hart¹⁷⁸ M. Heindl¹⁷⁸ D. Jaroslowski¹⁷⁸
 O. Karacheban^{178,ff} I. Laflotte¹⁷⁸ A. Lath¹⁷⁸ R. Montalvo,¹⁷⁸ K. Nash,¹⁷⁸ H. Routray¹⁷⁸ S. Salur¹⁷⁸

S. Schnetzer,¹⁷⁸ S. Somalwar,¹⁷⁸ R. Stone,¹⁷⁸ S. A. Thayil,¹⁷⁸ S. Thomas,¹⁷⁸ J. Vora,¹⁷⁸ H. Wang,¹⁷⁸ H. Acharya,¹⁷⁹ D. Ally,¹⁷⁹ A. G. Delanny,¹⁷⁹ S. Fiorendi,¹⁷⁹ T. Holmes,¹⁷⁹ N. Karunaratna,¹⁷⁹ L. Lee,¹⁷⁹ E. Nibigira,¹⁷⁹ S. Spanier,¹⁷⁹ D. Aebi,¹⁸⁰ M. Ahmad,¹⁸⁰ O. Bouhali,^{180,ssss} M. Dalchenko,¹⁸⁰ R. Eusebi,¹⁸⁰ J. Gilmore,¹⁸⁰ T. Huang,¹⁸⁰ T. Kamon,^{180,ttt} H. Kim,¹⁸⁰ S. Luo,¹⁸⁰ S. Malhotra,¹⁸⁰ R. Mueller,¹⁸⁰ D. Overton,¹⁸⁰ D. Rathjens,¹⁸⁰ A. Safonov,¹⁸⁰ N. Akchurin,¹⁸¹ J. Damgov,¹⁸¹ V. Hegde,¹⁸¹ A. Hussain,¹⁸¹ Y. Kazhykarim,¹⁸¹ K. Lamichhane,¹⁸¹ S. W. Lee,¹⁸¹ A. Mankel,¹⁸¹ T. Mengke,¹⁸¹ S. Muthumuni,¹⁸¹ T. Peltola,¹⁸¹ I. Volobouev,¹⁸¹ A. Whitbeck,¹⁸¹ E. Appelt,¹⁸² S. Greene,¹⁸² A. Gurrola,¹⁸² W. Johns,¹⁸² R. Kunnawalkam Elayavalli,¹⁸² A. Melo,¹⁸² F. Romeo,¹⁸² P. Sheldon,¹⁸² S. Tuo,¹⁸² J. Velkovska,¹⁸² J. Viinikainen,¹⁸² B. Cardwell,¹⁸³ B. Cox,¹⁸³ J. Hakala,¹⁸³ R. Hirosky,¹⁸³ A. Ledovskoy,¹⁸³ A. Li,¹⁸³ C. Neu,¹⁸³ C. E. Perez Lara,¹⁸³ P. E. Karchin,¹⁸⁴ A. Aravind,¹⁸⁵ S. Banerjee,¹⁸⁵ K. Black,¹⁸⁵ T. Bose,¹⁸⁵ S. Dasu,¹⁸⁵ I. De Bruyn,¹⁸⁵ P. Everaerts,¹⁸⁵ C. Galloni,¹⁸⁵ H. He,¹⁸⁵ M. Herndon,¹⁸⁵ A. Herve,¹⁸⁵ C. K. Koraka,¹⁸⁵ A. Lanaro,¹⁸⁵ R. Loveless,¹⁸⁵ J. Madhusudanan Sreekala,¹⁸⁵ A. Mallampalli,¹⁸⁵ A. Mohammadi,¹⁸⁵ S. Mondal,¹⁸⁵ G. Parida,¹⁸⁵ D. Pinna,¹⁸⁵ A. Savin,¹⁸⁵ V. Shang,¹⁸⁵ V. Sharma,¹⁸⁵ W. H. Smith,¹⁸⁵ D. Teague,¹⁸⁵ H. F. Tsoi,¹⁸⁵ W. Vetens,¹⁸⁵ A. Warden,¹⁸⁵ S. Afanasiev,¹⁸⁶ V. Andreev,¹⁸⁶ Yu. Andreev,¹⁸⁶ T. Aushev,¹⁸⁶ M. Azarkin,¹⁸⁶ A. Babaev,¹⁸⁶ A. Belyaev,¹⁸⁶ V. Blinov,^{186,q} E. Boos,¹⁸⁶ V. Borshch,¹⁸⁶ D. Budkouski,¹⁸⁶ V. Bunichev,¹⁸⁶ M. Chadeeva,^{186,q} V. Chekhovsky,¹⁸⁶ R. Chistov,^{186,q} A. Dermenev,¹⁸⁶ T. Dimova,^{186,q} D. Druzhkin,^{186,uuuu} M. Dubinin,^{186,llll} L. Dudko,¹⁸⁶ A. Ershov,¹⁸⁶ G. Gavrilo,¹⁸⁶ V. Gavrilo,¹⁸⁶ S. Gninenko,¹⁸⁶ V. Golovtcov,¹⁸⁶ N. Golubev,¹⁸⁶ I. Golutvin,¹⁸⁶ I. Gorbunov,¹⁸⁶ A. Gribushin,¹⁸⁶ Y. Ivanov,¹⁸⁶ V. Kachanov,¹⁸⁶ L. Kardapoltsev,^{186,q} V. Karjavine,¹⁸⁶ A. Karneyeu,¹⁸⁶ V. Kim,^{186,q} M. Kirakosyan,¹⁸⁶ D. Kirpichnikov,¹⁸⁶ M. Kirsanov,¹⁸⁶ V. Klyukhin,¹⁸⁶ D. Konstantinov,¹⁸⁶ V. Korenkov,¹⁸⁶ A. Kozyrev,^{186,q} N. Krasnikov,¹⁸⁶ A. Lanev,¹⁸⁶ P. Levchenko,^{186,vvvv} N. Lychkovskaya,¹⁸⁶ V. Makarenko,¹⁸⁶ A. Malakhov,¹⁸⁶ V. Matveev,^{186,q} V. Murzin,¹⁸⁶ A. Nikitenko,^{186,wwww,xxxx} S. Obraztsov,¹⁸⁶ V. Oreshkin,¹⁸⁶ V. Palichik,¹⁸⁶ V. Perelygin,¹⁸⁶ M. Perfilov,¹⁸⁶ S. Polikarpov,^{186,q} V. Popov,¹⁸⁶ O. Radchenko,^{186,q} M. Savina,¹⁸⁶ V. Savrin,¹⁸⁶ V. Shalaev,¹⁸⁶ S. Shmatov,¹⁸⁶ S. Shulha,¹⁸⁶ Y. Skovpen,^{186,q} S. Slabospitskii,¹⁸⁶ V. Smirnov,¹⁸⁶ D. Sosnov,¹⁸⁶ V. Sulimov,¹⁸⁶ E. Tcherniaev,¹⁸⁶ A. Terkulov,¹⁸⁶ O. Teryaev,^{186,a} I. Tlisova,¹⁸⁶ A. Toropin,¹⁸⁶ L. Uvarov,¹⁸⁶ A. Uzunian,¹⁸⁶ P. Volkov,¹⁸⁶ A. Vorobyev,^{186,a} G. Vorotnikov,¹⁸⁶ N. Voytishin,¹⁸⁶ B. S. Yuldashev,^{186,yyyy} A. Zarubin,¹⁸⁶ I. Zhizhin,¹⁸⁶ and A. Zhokin¹⁸⁶

(CMS Collaboration)

¹Yerevan Physics Institute, Yerevan, Armenia²Institut für Hochenergiephysik, Vienna, Austria³Universiteit Antwerpen, Antwerpen, Belgium⁴Vrije Universiteit Brussel, Brussel, Belgium⁵Université Libre de Bruxelles, Bruxelles, Belgium⁶Ghent University, Ghent, Belgium⁷Université Catholique de Louvain, Louvain-la-Neuve, Belgium⁸Centro Brasileiro de Pesquisas Físicas, Rio de Janeiro, Brazil⁹Universidade do Estado do Rio de Janeiro, Rio de Janeiro, Brazil¹⁰Universidade Estadual Paulista, Universidade Federal do ABC, São Paulo, Brazil¹¹Institute for Nuclear Research and Nuclear Energy, Bulgarian Academy of Sciences, Sofia, Bulgaria¹²University of Sofia, Sofia, Bulgaria¹³Instituto De Alta Investigación, Universidad de Tarapacá, Casilla 7 D, Arica, Chile¹⁴Beihang University, Beijing, China¹⁵Department of Physics, Tsinghua University, Beijing, China¹⁶Institute of High Energy Physics, Beijing, China¹⁷State Key Laboratory of Nuclear Physics and Technology, Peking University, Beijing, China¹⁸Sun Yat-Sen University, Guangzhou, China¹⁹University of Science and Technology of China, Hefei, China²⁰Institute of Modern Physics and Key Laboratory of Nuclear Physics and Ion-beam Application (MOE) - Fudan University, Shanghai, China²¹Zhejiang University, Hangzhou, Zhejiang, China²²Universidad de Los Andes, Bogota, Colombia

- ²³*Universidad de Antioquia, Medellin, Colombia*
- ²⁴*University of Split, Faculty of Electrical Engineering, Mechanical Engineering and Naval Architecture, Split, Croatia*
- ²⁵*University of Split, Faculty of Science, Split, Croatia*
- ²⁶*Institute Rudjer Boskovic, Zagreb, Croatia*
- ²⁷*University of Cyprus, Nicosia, Cyprus*
- ²⁸*Charles University, Prague, Czech Republic*
- ²⁹*Escuela Politecnica Nacional, Quito, Ecuador*
- ³⁰*Universidad San Francisco de Quito, Quito, Ecuador*
- ³¹*Academy of Scientific Research and Technology of the Arab Republic of Egypt, Egyptian Network of High Energy Physics, Cairo, Egypt*
- ³²*Center for High Energy Physics (CHEP-FU), Fayoum University, El-Fayoum, Egypt*
- ³³*National Institute of Chemical Physics and Biophysics, Tallinn, Estonia*
- ³⁴*Department of Physics, University of Helsinki, Helsinki, Finland*
- ³⁵*Helsinki Institute of Physics, Helsinki, Finland*
- ³⁶*Lappeenranta-Lahti University of Technology, Lappeenranta, Finland*
- ³⁷*IRFU, CEA, Université Paris-Saclay, Gif-sur-Yvette, France*
- ³⁸*Laboratoire Leprince-Ringuet, CNRS/IN2P3, Ecole Polytechnique, Institut Polytechnique de Paris, Palaiseau, France*
- ³⁹*Université de Strasbourg, CNRS, IPHC UMR 7178, Strasbourg, France*
- ⁴⁰*Institut de Physique des 2 Infinis de Lyon (IP2I), Villeurbanne, France*
- ⁴¹*Georgian Technical University, Tbilisi, Georgia*
- ⁴²*RWTH Aachen University, I. Physikalisches Institut, Aachen, Germany*
- ⁴³*RWTH Aachen University, III. Physikalisches Institut A, Aachen, Germany*
- ⁴⁴*RWTH Aachen University, III. Physikalisches Institut B, Aachen, Germany*
- ⁴⁵*Deutsches Elektronen-Synchrotron, Hamburg, Germany*
- ⁴⁶*University of Hamburg, Hamburg, Germany*
- ⁴⁷*Karlsruher Institut fuer Technologie, Karlsruhe, Germany*
- ⁴⁸*Institute of Nuclear and Particle Physics (INPP), NCSR Demokritos, Aghia Paraskevi, Greece*
- ⁴⁹*National and Kapodistrian University of Athens, Athens, Greece*
- ⁵⁰*National Technical University of Athens, Athens, Greece*
- ⁵¹*University of Ioánnina, Ioánnina, Greece*
- ⁵²*HUN-REN Wigner Research Centre for Physics, Budapest, Hungary*
- ⁵³*MTA-ELTE Lendület CMS Particle and Nuclear Physics Group, Eötvös Loránd University, Budapest, Hungary*
- ⁵⁴*Faculty of Informatics, University of Debrecen, Debrecen, Hungary*
- ⁵⁵*Institute of Nuclear Research ATOMKI, Debrecen, Hungary*
- ⁵⁶*Karoly Robert Campus, MATE Institute of Technology, Gyongyos, Hungary*
- ⁵⁷*Panjab University, Chandigarh, India*
- ⁵⁸*University of Delhi, Delhi, India*
- ⁵⁹*Saha Institute of Nuclear Physics, HBNI, Kolkata, India*
- ⁶⁰*Indian Institute of Technology Madras, Madras, India*
- ⁶¹*Tata Institute of Fundamental Research-A, Mumbai, India*
- ⁶²*Tata Institute of Fundamental Research-B, Mumbai, India*
- ⁶³*National Institute of Science Education and Research, An OCC of Homi Bhabha National Institute, Bhubaneswar, Odisha, India*
- ⁶⁴*Indian Institute of Science Education and Research (IISER), Pune, India*
- ⁶⁵*Isfahan University of Technology, Isfahan, Iran*
- ⁶⁶*Institute for Research in Fundamental Sciences (IPM), Tehran, Iran*
- ⁶⁷*University College Dublin, Dublin, Ireland*
- ^{68a}*INFN Sezione di Bari, Bari, Italy*
- ^{68b}*Università di Bari, Bari, Italy*
- ^{68c}*Politecnico di Bari, Bari, Italy*
- ^{69a}*INFN Sezione di Bologna, Bologna, Italy*
- ^{69b}*Università di Bologna, Bologna, Italy*
- ^{70a}*INFN Sezione di Catania, Catania, Italy*
- ^{70b}*Università di Catania, Catania, Italy*
- ^{71a}*INFN Sezione di Firenze, Firenze, Italy*
- ^{71b}*Università di Firenze, Firenze, Italy*
- ⁷²*INFN Laboratori Nazionali di Frascati, Frascati, Italy*

- ^{73a}INFN Sezione di Genova, Genova, Italy
^{73b}Università di Genova, Genova, Italy
^{74a}INFN Sezione di Milano-Bicocca, Milano, Italy
^{74b}Università di Milano-Bicocca, Milano, Italy
^{75a}INFN Sezione di Napoli, Napoli, Italy
^{75b}Università di Napoli 'Federico II', Napoli, Italy
^{75c}Università della Basilicata, Potenza, Italy
^{75d}Scuola Superiore Meridionale (SSM), Napoli, Italy
^{76a}INFN Sezione di Padova, Padova, Italy
^{76b}Università di Padova, Padova, Italy
^{76c}Università di Trento, Trento, Italy
^{77a}INFN Sezione di Pavia, Pavia, Italy
^{77b}Università di Pavia, Pavia, Italy
^{78a}INFN Sezione di Perugia, Perugia, Italy
^{78b}Università di Perugia, Perugia, Italy
^{79a}INFN Sezione di Pisa, Pisa, Italy
^{79b}Università di Pisa, Pisa, Italy
^{79c}Scuola Normale Superiore di Pisa, Pisa, Italy
^{79d}Università di Siena, Siena, Italy
^{80a}INFN Sezione di Roma, Roma, Italy
^{80b}Sapienza Università di Roma, Roma, Italy
^{81a}INFN Sezione di Torino, Torino, Italy
^{81b}Università di Torino, Torino, Italy
^{81c}Università del Piemonte Orientale, Novara, Italy
^{82a}INFN Sezione di Trieste, Trieste, Italy
^{82b}Università di Trieste, Trieste, Italy
⁸³Kyungpook National University, Daegu, Korea
⁸⁴Department of Mathematics and Physics - GWNNU, Gangneung, Korea
⁸⁵Chonnam National University, Institute for Universe and Elementary Particles, Kwangju, Korea
⁸⁶Hanyang University, Seoul, Korea
⁸⁷Korea University, Seoul, Korea
⁸⁸Kyung Hee University, Department of Physics, Seoul, Korea
⁸⁹Sejong University, Seoul, Korea
⁹⁰Seoul National University, Seoul, Korea
⁹¹University of Seoul, Seoul, Korea
⁹²Yonsei University, Department of Physics, Seoul, Korea
⁹³Sungkyunkwan University, Suwon, Korea
⁹⁴College of Engineering and Technology, American University of the Middle East (AUM),
 Dasman, Kuwait
⁹⁵Riga Technical University, Riga, Latvia
⁹⁶University of Latvia (LU), Riga, Latvia
⁹⁷Vilnius University, Vilnius, Lithuania
⁹⁸National Centre for Particle Physics, Universiti Malaya, Kuala Lumpur, Malaysia
⁹⁹Universidad de Sonora (UNISON), Hermosillo, Mexico
¹⁰⁰Centro de Investigación y de Estudios Avanzados del IPN, Mexico City, Mexico
¹⁰¹Universidad Iberoamericana, Mexico City, Mexico
¹⁰²Benemerita Universidad Autónoma de Puebla, Puebla, Mexico
¹⁰³University of Montenegro, Podgorica, Montenegro
¹⁰⁴University of Canterbury, Christchurch, New Zealand
¹⁰⁵National Centre for Physics, Quaid-I-Azam University, Islamabad, Pakistan
¹⁰⁶AGH University of Krakow, Faculty of Computer Science, Electronics and Telecommunications,
 Krakow, Poland
¹⁰⁷National Centre for Nuclear Research, Swierk, Poland
¹⁰⁸Institute of Experimental Physics, Faculty of Physics, University of Warsaw, Warsaw, Poland
¹⁰⁹Warsaw University of Technology, Warsaw, Poland
¹¹⁰Laboratório de Instrumentação e Física Experimental de Partículas, Lisboa, Portugal
¹¹¹Faculty of Physics, University of Belgrade, Belgrade, Serbia
¹¹²VINCA Institute of Nuclear Sciences, University of Belgrade, Belgrade, Serbia
¹¹³Centro de Investigaciones Energéticas Medioambientales y Tecnológicas (CIEMAT), Madrid, Spain
¹¹⁴Universidad Autónoma de Madrid, Madrid, Spain

- ¹¹⁵*Universidad de Oviedo, Instituto Universitario de Ciencias y Tecnologías Espaciales de Asturias (ICTEA), Oviedo, Spain*
- ¹¹⁶*Instituto de Física de Cantabria (IFCA), CSIC-Universidad de Cantabria, Santander, Spain*
- ¹¹⁷*University of Colombo, Colombo, Sri Lanka*
- ¹¹⁸*University of Ruhuna, Department of Physics, Matara, Sri Lanka*
- ¹¹⁹*CERN, European Organization for Nuclear Research, Geneva, Switzerland*
- ¹²⁰*Paul Scherrer Institut, Villigen, Switzerland*
- ¹²¹*ETH Zurich - Institute for Particle Physics and Astrophysics (IPA), Zurich, Switzerland*
- ¹²²*Universität Zürich, Zurich, Switzerland*
- ¹²³*National Central University, Chung-Li, Taiwan*
- ¹²⁴*National Taiwan University (NTU), Taipei, Taiwan*
- ¹²⁵*High Energy Physics Research Unit, Department of Physics, Faculty of Science, Chulalongkorn University, Bangkok, Thailand*
- ¹²⁶*Çukurova University, Physics Department, Science and Art Faculty, Adana, Turkey*
- ¹²⁷*Middle East Technical University, Physics Department, Ankara, Turkey*
- ¹²⁸*Bogazici University, Istanbul, Turkey*
- ¹²⁹*Istanbul Technical University, Istanbul, Turkey*
- ¹³⁰*Istanbul University, Istanbul, Turkey*
- ¹³¹*Institute for Scintillation Materials of National Academy of Science of Ukraine, Kharkiv, Ukraine*
- ¹³²*National Science Centre, Kharkiv Institute of Physics and Technology, Kharkiv, Ukraine*
- ¹³³*University of Bristol, Bristol, United Kingdom*
- ¹³⁴*Rutherford Appleton Laboratory, Didcot, United Kingdom*
- ¹³⁵*Imperial College, London, United Kingdom*
- ¹³⁶*Brunel University, Uxbridge, United Kingdom*
- ¹³⁷*Baylor University, Waco, Texas, USA*
- ¹³⁸*Catholic University of America, Washington, DC, USA*
- ¹³⁹*The University of Alabama, Tuscaloosa, Alabama, USA*
- ¹⁴⁰*Boston University, Boston, Massachusetts, USA*
- ¹⁴¹*Brown University, Providence, Rhode Island, USA*
- ¹⁴²*University of California, Davis, Davis, California, USA*
- ¹⁴³*University of California, Los Angeles, California, USA*
- ¹⁴⁴*University of California, Riverside, Riverside, California, USA*
- ¹⁴⁵*University of California, San Diego, La Jolla, California, USA*
- ¹⁴⁶*University of California, Santa Barbara - Department of Physics, Santa Barbara, California, USA*
- ¹⁴⁷*California Institute of Technology, Pasadena, California, USA*
- ¹⁴⁸*Carnegie Mellon University, Pittsburgh, Pennsylvania, USA*
- ¹⁴⁹*University of Colorado Boulder, Boulder, Colorado, USA*
- ¹⁵⁰*Cornell University, Ithaca, New York, USA*
- ¹⁵¹*Fermi National Accelerator Laboratory, Batavia, Illinois, USA*
- ¹⁵²*University of Florida, Gainesville, Florida, USA*
- ¹⁵³*Florida State University, Tallahassee, Florida, USA*
- ¹⁵⁴*Florida Institute of Technology, Melbourne, Florida, USA*
- ¹⁵⁵*University of Illinois Chicago, Chicago, USA, Chicago, USA*
- ¹⁵⁶*The University of Iowa, Iowa City, Iowa, USA*
- ¹⁵⁷*Johns Hopkins University, Baltimore, Maryland, USA*
- ¹⁵⁸*The University of Kansas, Lawrence, Kansas, USA*
- ¹⁵⁹*Kansas State University, Manhattan, Kansas, USA*
- ¹⁶⁰*Lawrence Livermore National Laboratory, Livermore, California, USA*
- ¹⁶¹*University of Maryland, College Park, Maryland, USA*
- ¹⁶²*Massachusetts Institute of Technology, Cambridge, Massachusetts, USA*
- ¹⁶³*University of Minnesota, Minneapolis, Minnesota, USA*
- ¹⁶⁴*University of Mississippi, Oxford, Mississippi, USA*
- ¹⁶⁵*University of Nebraska-Lincoln, Lincoln, Nebraska, USA*
- ¹⁶⁶*State University of New York at Buffalo, Buffalo, New York, USA*
- ¹⁶⁷*Northeastern University, Boston, Massachusetts, USA*
- ¹⁶⁸*Northwestern University, Evanston, Illinois, USA*
- ¹⁶⁹*University of Notre Dame, Notre Dame, Indiana, USA*
- ¹⁷⁰*The Ohio State University, Columbus, Ohio, USA*
- ¹⁷¹*Princeton University, Princeton, New Jersey, USA*
- ¹⁷²*University of Puerto Rico, Mayaguez, Puerto Rico, USA*

- ¹⁷³*Purdue University, West Lafayette, Indiana, USA*
¹⁷⁴*Purdue University Northwest, Hammond, Indiana, USA*
¹⁷⁵*Rice University, Houston, Texas, USA*
¹⁷⁶*University of Rochester, Rochester, New York, USA*
¹⁷⁷*The Rockefeller University, New York, New York, USA*
¹⁷⁸*Rutgers, The State University of New Jersey, Piscataway, New Jersey, USA*
¹⁷⁹*University of Tennessee, Knoxville, Tennessee, USA*
¹⁸⁰*Texas A&M University, College Station, Texas, USA*
¹⁸¹*Texas Tech University, Lubbock, Texas, USA*
¹⁸²*Vanderbilt University, Nashville, Tennessee, USA*
¹⁸³*University of Virginia, Charlottesville, Virginia, USA*
¹⁸⁴*Wayne State University, Detroit, Michigan, USA*
¹⁸⁵*University of Wisconsin - Madison, Madison, Wisconsin, USA*
¹⁸⁶*An institute or international laboratory covered by a cooperation agreement with CERN*

^aDeceased.

^bAlso at Yerevan State University, Yerevan, Armenia.

^cAlso at TU Wien, Vienna, Austria.

^dAlso at Institute of Basic and Applied Sciences, Faculty of Engineering, Arab Academy for Science, Technology and Maritime Transport, Alexandria, Egypt.

^eAlso at Ghent University, Ghent, Belgium.

^fAlso at Universidade Estadual de Campinas, Campinas, Brazil.

^gAlso at Federal University of Rio Grande do Sul, Porto Alegre, Brazil.

^hAlso at UFMS, Nova Andradina, Brazil.

ⁱAlso at Nanjing Normal University, Nanjing, China.

^jAlso at Henan Normal University, Xinxiang, China.

^kAlso at The University of Iowa, Iowa City, Iowa, USA.

^lAlso at University of Chinese Academy of Sciences, Beijing, China.

^mAlso at China Center of Advanced Science and Technology, Beijing, China.

ⁿAlso at University of Chinese Academy of Sciences, Beijing, China.

^oAlso at China Spallation Neutron Source, Guangdong, China.

^pAlso at Université Libre de Bruxelles, Bruxelles, Belgium.

^qAlso at Another institute or international laboratory covered by a cooperation agreement with CERN.

^rAlso at Helwan University, Cairo, Egypt.

^sAlso at Zewail City of Science and Technology, Zewail, Egypt.

^tAlso at British University in Egypt, Cairo, Egypt.

^uAlso at Ain Shams University, Cairo, Egypt.

^vAlso at Birla Institute of Technology, Mesra, Mesra, India.

^wAlso at Purdue University, West Lafayette, Indiana, USA.

^xAlso at Université de Haute Alsace, Mulhouse, France.

^yAlso at Department of Physics, Tsinghua University, Beijing, China.

^zAlso at The University of the State of Amazonas, Manaus, Brazil.

^{aa}Also at Erzincan Binali Yildirim University, Erzincan, Turkey.

^{bb}Also at University of Hamburg, Hamburg, Germany.

^{cc}Also at RWTH Aachen University, III. Physikalisches Institut A, Aachen, Germany.

^{dd}Also at Isfahan University of Technology, Isfahan, Iran.

^{ee}Also at Bergische University Wuppertal (BUW), Wuppertal, Germany.

^{ff}Also at Brandenburg University of Technology, Cottbus, Germany.

^{gg}Also at Forschungszentrum Jülich, Juelich, Germany.

^{hh}Also at CERN, European Organization for Nuclear Research, Geneva, Switzerland.

ⁱⁱAlso at Institute of Physics, University of Debrecen, Debrecen, Hungary.

^{jj}Also at Institute of Nuclear Research ATOMKI, Debrecen, Hungary.

^{kk}Also at Universitatea Babeş-Bolyai—Facultatea de Fizica, Cluj-Napoca, Romania.

^{ll}Also at Physics Department, Faculty of Science, Assiut University, Assiut, Egypt.

^{mm}Also at HUN-REN Wigner Research Centre for Physics, Budapest, Hungary.

ⁿⁿAlso at Faculty of Informatics, University of Debrecen, Debrecen, Hungary.

^{oo}Also at Punjab Agricultural University, Ludhiana, India.

^{pp}Also at University of Hyderabad, Hyderabad, India.

^{qq}Also at University of Visva-Bharati, Santiniketan, India.

^{rr}Also at Indian Institute of Science (IISc), Bangalore, India.

- ^{ss} Also at IIT Bhubaneswar, Bhubaneswar, India.
- ^{tt} Also at Institute of Physics, Bhubaneswar, India.
- ^{uu} Also at Deutsches Elektronen-Synchrotron, Hamburg, Germany.
- ^{vv} Also at Department of Physics, Isfahan University of Technology, Isfahan, Iran.
- ^{ww} Also at Sharif University of Technology, Tehran, Iran.
- ^{xx} Also at Department of Physics, University of Science and Technology of Mazandaran, Behshahr, Iran.
- ^{yy} Also at Italian National Agency for New Technologies, Energy and Sustainable Economic Development, Bologna, Italy.
- ^{zz} Also at Centro Siciliano di Fisica Nucleare e di Struttura Della Materia, Catania, Italy.
- ^{aaa} Also at Università degli Studi Guglielmo Marconi, Roma, Italy.
- ^{bbb} Also at Scuola Superiore Meridionale, Università di Napoli 'Federico II', Napoli, Italy.
- ^{ccc} Also at Fermi National Accelerator Laboratory, Batavia, Illinois, USA.
- ^{ddd} Also at Università di Napoli 'Federico II', Napoli, Italy.
- ^{eee} Also at Consiglio Nazionale delle Ricerche—Istituto Officina dei Materiali, Perugia, Italy.
- ^{fff} Also at Riga Technical University, Riga, Latvia.
- ^{ggg} Also at Department of Applied Physics, Faculty of Science and Technology, Universiti Kebangsaan Malaysia, Bangi, Malaysia.
- ^{hhh} Also at Consejo Nacional de Ciencia y Tecnología, Mexico City, Mexico.
- ⁱⁱⁱ Also at Trincomalee Campus, Eastern University, Sri Lanka, Nilaveli, Sri Lanka.
- ^{jjj} Also at Saegis Campus, Nugegoda, Sri Lanka.
- ^{kkk} Also at INFN Sezione di Pavia, Università di Pavia, Pavia, Italy.
- ^{lll} Also at National and Kapodistrian University of Athens, Athens, Greece.
- ^{mmm} Also at Ecole Polytechnique Fédérale Lausanne, Lausanne, Switzerland.
- ⁿⁿⁿ Also at University of Vienna Faculty of Computer Science, Vienna, Austria.
- ^{ooo} Also at Universität Zürich, Zurich, Switzerland.
- ^{ppp} Also at Stefan Meyer Institute for Subatomic Physics, Vienna, Austria.
- ^{qqq} Also at Laboratoire d'Annecy-le-Vieux de Physique des Particules, IN2P3-CNRS, Annecy-le-Vieux, France.
- ^{rrr} Also at Near East University, Research Center of Experimental Health Science, Mersin, Turkey.
- ^{sss} Also at Konya Technical University, Konya, Turkey.
- ^{ttt} Also at Izmir Bakircay University, Izmir, Turkey.
- ^{uuu} Also at Adiyaman University, Adiyaman, Turkey.
- ^{vvv} Also at Bozok Universitetesi Rektörlüğü, Yozgat, Turkey.
- ^{www} Also at Marmara University, Istanbul, Turkey.
- ^{xxx} Also at Milli Savunma University, Istanbul, Turkey.
- ^{yyy} Also at Kafkas University, Kars, Turkey.
- ^{zzz} Also at stanbul Okan University, Istanbul, Turkey.
- ^{aaaa} Also at Hacettepe University, Ankara, Turkey.
- ^{bbbb} Also at Istanbul University—Cerrahpasa, Faculty of Engineering, Istanbul, Turkey.
- ^{cccc} Also at Yildiz Technical University, Istanbul, Turkey.
- ^{dddd} Also at Vrije Universiteit Brussel, Brussel, Belgium.
- ^{eeee} Also at School of Physics and Astronomy, University of Southampton, Southampton, United Kingdom.
- ^{ffff} Also at University of Bristol, Bristol, United Kingdom.
- ^{gggg} Also at IPPP Durham University, Durham, United Kingdom.
- ^{hhhh} Also at Monash University, Faculty of Science, Clayton, Australia.
- ⁱⁱⁱⁱ Also at Università di Torino, Torino, Italy.
- ^{jjjj} Also at Bethel University, St. Paul, Minnesota, USA.
- ^{kkkk} Also at Karamanoğlu Mehmetbey University, Karaman, Turkey.
- ^{llll} Also at California Institute of Technology, Pasadena, California, USA.
- ^{mmmm} Also at United States Naval Academy, Annapolis, Maryland, USA.
- ⁿⁿⁿⁿ Also at Bingol University, Bingol, Turkey.
- ^{oooo} Also at Georgian Technical University, Tbilisi, Georgia.
- ^{pppp} Also at Sinop University, Sinop, Turkey.
- ^{qqqq} Also at Erciyes University, Kayseri, Turkey.
- ^{rrrr} Also at Horia Hulubei National Institute of Physics and Nuclear Engineering (IFIN-HH), Bucharest, Romania.
- ^{ssss} Also at Texas A&M University at Qatar, Doha, Qatar.
- ^{tttt} Also at Kyungpook National University, Daegu, Korea.
- ^{uuuu} Also at Universiteit Antwerpen, Antwerpen, Belgium.
- ^{vvvv} Also at Northeastern University, Boston, Massachusetts, USA.
- ^{wwww} Also at Imperial College, London, United Kingdom.
- ^{xxxx} Also at Yerevan Physics Institute, Yerevan, Armenia.
- ^{yyyy} Also at Institute of Nuclear Physics of the Uzbekistan Academy of Sciences, Tashkent, Uzbekistan.